

Boosting Propagule Transport Models with Individual-Specific Data from Mobile Apps

Samuel M. Fischer^{1,2,*}, Pouria Ramazi³, Sean Simmons⁴, Mark S. Poesch⁵, and Mark A.
Lewis^{1,6}

¹*Department of Mathematical and Statistical Sciences, University of Alberta, Edmonton, AB, T6G 2G1, Canada.*

²*Department of Ecological Modelling, Helmholtz-Centre for Environmental Research - UFZ, Permoserstraße 15, 04318 Leipzig, Germany.*

³*Department of Mathematics and Statistics, Brock University, St. Catharines, ON, L2S 3A1, Canada.*

⁴*Angler's Atlas, Goldstream Publishing, PO Box 182, Prince George, BC, V2L 4S1, Canada.*

⁵*Department of Renewable Resources, University of Alberta, Edmonton, AB, T6G 2R3, Canada.*

⁶*Department of Biological Sciences, University of Alberta, Edmonton, AB, T6G 2E9, Canada.*

* *samuel.fischer@ualberta.ca*

Abstract

1. Management of invasive species and pathogens requires information about the traffic of potential vectors. Such information is often taken from vector traffic models fitted to survey data. Here, user-specific data collected via mobile apps offer new opportunities to obtain more accurate estimates and to analyze how vectors' individual preferences affect propagule flows. However, data voluntarily reported via apps may lack some trip records, adding a significant layer of uncertainty. We show how the benefits of app-based data can be exploited despite this drawback.
2. Based on data collected via an angler app, we built a stochastic model for angler traffic in the Canadian province Alberta. There, anglers facilitate the spread of whirling disease, a parasite-induced fish disease. The model is temporally and spatially explicit and accounts for individual preferences and repeating behaviour of anglers, helping to address the problem of missing trip records.
3. We obtained estimates of angler traffic between all subbasins in Alberta. The model's accuracy exceeds that of direct empirical estimates even when fewer data were used to fit

the model. The results indicate that anglers' local preferences and their tendency to revisit previous destinations reduce the number of long inter-waterbody trips potentially dispersing whirling disease. According to our model, anglers revisit their previous destination in 64% of their trips, making these trips irrelevant for the spread of whirling disease. Furthermore, 54% of fishing trips end in individual-specific spatially contained areas with mean radius of 54.7 km. Finally, although the fraction of trips that anglers report was unknown, we were able to estimate the total yearly number of fishing trips in Alberta, matching an independent empirical estimate.

4. **Policy implications:** We make two major contributions: (1) we provide a model that uses mobile app data to boost the mechanistic accuracy of classic propagule transport models, and (2) we demonstrate the importance of individual-specific behaviour of vectors for propagule transport. Ignoring vectors' local preferences and their tendency to revisit previous destinations can lead to significant overestimates of vector traffic and biased estimates of propagule flows. This has clear implications for the management of invasive species and animal diseases.

Keywords: Angler; Gravity Model; Invasives (Applied Ecology); Modelling (Disease Ecology); Smartphone Apps; Survey Method; Vector; Whirling Disease.

1 Introduction

Recreational overland traffic is a major vector for several invasive species and pathogens (Karesh *et al.*, 2005; Hulme, 2009). Examples include invasive plants and pathogens carried via the soil attached to gear and vehicles of tourists (Von der Lippe & Kowarik, 2007; Cushman & Meentemeyer, 2008), invasive insects introduced along with campers' firewood (Koch *et al.*, 2012), or invasive mussels, non-indigenous bait fish, and water-borne diseases spread by recreational boaters (Johnson *et al.*, 2001) and anglers (Nalepa & Schloesser, 2013; Litvak & Mandrak, 1993; Kilian *et al.*, 2012; Gates *et al.*, 2007). Given the difficulties and costs associated with eradicating invasive species and pathogens once they have established at a site, it is key that any management strategy prevents propagule transport and detects new infestations early (Leung & Mandrak, 2007; Pluess *et al.*, 2012). This requires a detailed understanding of transport pathways and vector's movement patterns.

Data collected via smartphone apps have become a valuable resource to study human mobility

(Wang *et al.*, 2019) and offer new opportunities to understand and predict the dispersal of invasive species and pathogens (Papenfuss *et al.*, 2015; Venturelli *et al.*, 2017). Assuming a sufficiently large user base, mobile app data can be collected at relatively low cost over large spatial and temporal scales (Papenfuss *et al.*, 2015; Venturelli *et al.*, 2017). However, even if many trip records are available, the datasets collected via apps are typically far from complete: often, only a small fraction of the population of interest, e.g. hikers or anglers, use any particular app, and app users do not record all their trips (Papenfuss *et al.*, 2015). Even if an app records thousands of trips, this number remains small in comparison to the vast number of origin-destination pairs for which traffic estimates may be desired. For example, if we seek to estimate the vector traffic between 100 origins and 100 destinations, the number of origin-destination *pairs* is 10 000. Hence, direct empirical estimates of traffic flows can be prone to significant statistical error.

A common approach to bridge such data gaps is to use models, such as gravity models (Bossenbroek *et al.*, 2001; Ferrari *et al.*, 2006; Potapov *et al.*, 2010; Muirhead & MacIsaac, 2011; Li *et al.*, 2011). By combining empirical observations with additional covariates, e.g. geographical and socio-economic data, models can provide detailed estimates of vector traffic on broad scales and may even allow insights into the mechanisms behind traffic patterns. In the past, vector traffic models have been fitted to data collected via mail-out surveys (Potapov *et al.*, 2010; Muirhead & MacIsaac, 2011; Chivers & Leung, 2012; Drake & Mandrak, 2014), roadside traffic surveys (Fischer *et al.*, 2020), on-site surveys at origins and destinations (Leung *et al.*, 2004; Bossenbroek *et al.*, 2007), or registration records from origins and destinations (Bossenbroek *et al.*, 2001; Prasad *et al.*, 2010). However, since gathering data via these methods is often costly and the data may represent specific locations and time frames only, app data are a promising alternative resource for fitting vector traffic models. In this study, we show how this can be done.

A drawback of app data is that app users may report their trips sparsely, making the temporal sequence of their trips incomplete. The data may still yield insight into how often each destination is visited, but without knowing the full trip sequence, it is difficult to gauge how far and quickly vectors will spread propagules after being infested. A vector frequently revisiting their previous destination has a much lower risk of spreading a disease than a vector who prefers to alternate between destinations. As the risk of a successful transmission is highest between consecutively visited sites, disregarding the trips not recorded by app users could bias the predictions of propagule

dispersion models significantly.

To estimate the number of relevant trips between sites despite missing data, some studies assume that the destinations of consecutive trips are chosen independently from one another (Bossenbroek *et al.*, 2001; Leung *et al.*, 2004). Then, incomplete trip sequences would be representative for all trips. In practice, however, individual travellers may have local preferences and tend to revisit previous destinations, which would lower the risk of propagule transport. Accounting for these individual preferences requires a more intricate modelling approach. We tackle this problem and build a vector movement model that can be fitted to incomplete app-based data.

Though our approach is applicable to studying the spread of various pests in both terrestrial and aquatic systems, we introduce and demonstrate it by considering a particular case study: we model angler movement in the Canadian province Alberta based on data collected via the “MyCatch” angler app so as to create a risk map for the spread of whirling disease in Alberta. Our focal invader, whirling disease, is a fish disease caused by the aquatic parasite *M. cerebralis* (Hofer, 1903), which can increase the death rate of juvenile salmonid fish up to 90% (Elwell *et al.*, 2010) and may thus entail severe ecological and economic consequences (Turner *et al.*, 2014; Ramazi *et al.*, 2021a). As there is currently no known cure for whirling disease in natural ecosystems (Turner *et al.*, 2014), management is limited to reducing the risk of parasite introduction.

Our main objective is to estimate how often each subbasin in Alberta is visited by anglers who have visited an infested area on their previous trip. Whilst estimating angler traffic, we also assess how traffic depends on local preferences of individual anglers and their tendency to revisit previous destinations. Our results indicate that if these factors are not accounted for, local traffic is significantly underestimated while long-distance traffic is overestimated. This, in turn, has general implications for risk assessment and management of invasive species and infectious diseases.

2 Materials and Methods

An overview of the data and submodels used in our approach is displayed in Figure 1. Below we describe the components and their interplay in detail. An overview of the mathematical symbols used in this paper is provided in Appendix S1 in Supporting Information.

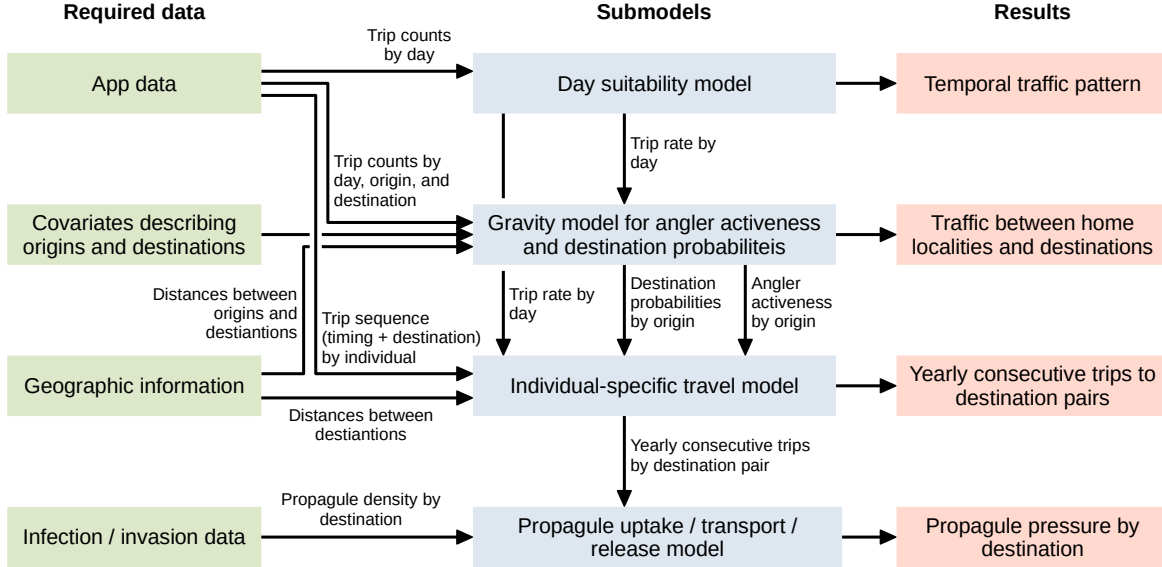


Figure 1: Model components. The data required for the analysis are displayed in green, the different submodels in blue, and the results in red. The submodels are combined into a stochastic traffic model described in section 2.2. Though incorporating a sophisticated propagule transport model is possible, we use the number of directly consecutive trips from infested to uninfested areas as a proxy for propagule pressure in this study.

2.1 Data

We used a dataset collected via the MyCatch angler app, which can be downloaded free of charge for Android and iOS devices and allows anglers to share information regarding waterbodies they visit, e.g. their catch success. App users need to provide their home postal codes and may record their fishing destinations either via GPS or select their destination waterbodies on a map. In addition to using the app, registered users can also enter information via a web interface. Though not all anglers in Alberta use the app, the app users have been found to be mostly representative of the province’s anglers, with a slight bias towards higher app usage in urban areas (Johnston *et al.*, 2021).

The data were collected from May 2018 to April 2020 inclusive. We determined the home *locality* (city, town, village, etc.) of each app user who recorded at least one trip within this time frame and collected the sequence of their fishing destinations along with the trip dates. If an angler recorded several trips to the same waterbody on a day, we merged these into a single trip. To keep the number of fishing destinations tractable, we aggregated them over *subbasins* (hydrologic units of level 8) and neglected more detailed information. Subbasins are a natural unit for modelling the spread

Group	Covariate	Median	Maximum
Angler activeness in localities	Locality population (2019)	$0.34 \cdot 10^3$	$1\,286 \cdot 10^3$
	Mean income (2013)	36 900 CAD	99 600 CAD
	Median income (2013)	34 600 CAD	78 100 CAD
Fishing opportunities in subbasins	Total perimeter of waterbodies	350 km	1 570 km
	Total area of waterbodies	4 km ²	2 160 km ²
	Total perimeter with confirmed species	0 km	620 km
	Total area with confirmed species	0 km ²	1 390 km ²
Infrastructure in subbasins	Population in 10 km range (2019)	$0.4 \cdot 10^3$	$1\,394 \cdot 10^3$
	Public campgrounds in 10 km range	1	19
Social media presence of subbasins	Total species upvotes (2018 – 2019)	0	196
	Total waterbody web page visits (2018 – 2019)	140	21 945

Table 1: Considered covariates and their median and maximum values.

of aquatic diseases, because they have a unique outflow each. Alberta consists of 422 subbasins with a mean area of 1517 km². Our dataset included 575 anglers, who made 2104 trips. For 229 of these trips, we could not determine the destination subbasin, because the anglers did not provide destination coordinates and the reported destination waterbodies spanned multiple subbasins. We disregarded these trips. All research was conducted in accordance with the Human Research Ethics Policy of the University of Alberta (approval number Pro00102610).

As predictors for anglers’ behaviour, we used data on the localities and the subbasins (Table 1). Besides geographical and socioeconomic data, we compiled data collected on the Angler’s Atlas website (www.anglersatlas.com). The website contains a page for each major waterbody in Alberta, providing anglers with waterbody-specific information and allowing them to report the species of fish they have caught there. Fish species reports can be upvoted and downvoted by other anglers to confirm or rebut an observation. We computed for each subbasin the area and perimeter of all waterbodies with at least one confirmed fish species. Furthermore, we computed the cumulative number of waterbody webpage visits and species upvotes per subbasin. For waterbodies spanning over multiple subbasins, we distributed the values over all applicable units according to their share of the waterbodies’ perimeters. In addition to the listed covariates, we determined the number of registered anglers for each locality. The sources of the individual datasets we used are listed in the Data Sources section.

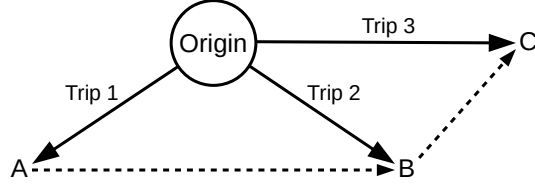


Figure 2: Possible sequence of trips to the destinations A , B , and C for an angler with home locality “origin”. The risk that the angler transports propagules or pathogens is highest for consecutively visited fishing locations, i.e. for destinations A and B and for B and C . Our goal is to estimate the number of such consecutive fishing trips for any pair of destinations. Our dataset contains information on individual trips, but some trips may not have been recorded.

2.2 Angler traffic as a stochastic process

We modelled anglers’ decision-making as a stochastic process, which determines both the *recorded* number of fishing trips between each home locality and subbasin (*origin* and *destination*) and the *expected* yearly number $\mu_{j_1 j_2}$ of trips anglers make to destination j_1 directly after visiting destination j_2 . While we sought to estimate the latter number for all destination pairs, we fitted the model based on the former (Figure 2).

We assumed that anglers start all their fishing trips at their home localities and visit a single destination per trip. They make trips randomly at rates dependent on their origins, the date, and random factors not explicitly covered in the model, e.g. weather conditions. We modelled the trip rate for an angler from origin i on day t as $\mu_i \varepsilon_t$, where the *angler activeness* μ_i is the mean number of trips per day for an angler from origin i , and the *day suitability* ε_t is a gamma random variable with mean τ_t , denoting how well day t of the study period is suited for going fishing:

$$\varepsilon_t \sim \text{Gamma}\left(\frac{\tau_t}{\alpha}, \alpha\right). \quad (1)$$

The gamma distribution can take on a variety of shapes and is thus suited for diverse modelling applications (Kleiber & Kotz, 2003; Husak *et al.*, 2007). The dispersion parameter α determines the variance of the day suitability; the expected day suitability τ_t is normalized so that its temporal average is 1, i.e. $\frac{1}{T} \sum_t \tau_t = 1$ with T being the number of days in the study period. We supposed that the day suitability ε_t is the same for all anglers in Alberta, whereas their individual decisions

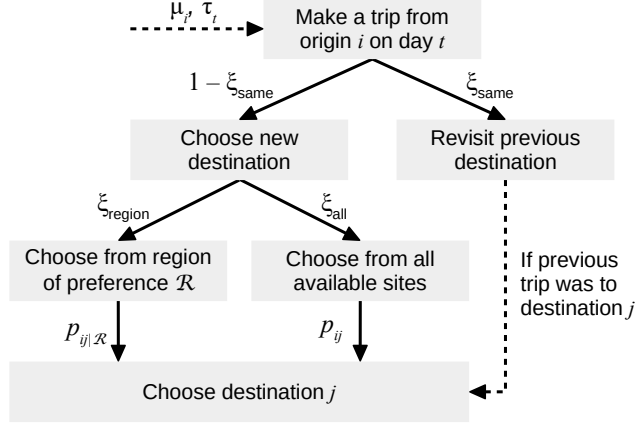


Figure 3: Visualization of anglers’ decision-making process. The parameters μ_i and τ_t determine the expected rate at which anglers from origin i make trips on day t . When an angler chooses their destination, they may revisit their previous destination with probability ξ_{same} . Otherwise, they may either constrain their choice to their region of preference (with probability ξ_{region}) or make an unconstrained selection from all available destinations (with probability ξ_{all}). If they decide to constrain their choice to their region of preference \mathcal{R} , they choose destination j with probability $p_{ij|\mathcal{R}}$. Otherwise, they choose it with probability p_{ij} .

are independent from one another. The values μ_i and τ_t are given by the submodels in section 2.4.

We assumed that anglers choose the destinations of their trips based on individual local preferences and their previous fishing destinations (Figures 3, 4). Consider an angler from origin i . With probability ξ_{same} , they decide to revisit the destination of their last trip. Otherwise, they choose a new destination as follows: with probability ξ_{region} , they constrain their destination choice to their *region of preference* \mathcal{R} – a spatially contained set of destinations that they personally like best – and choose a destination $j \in \mathcal{R}$ according to probabilities $p_{ij|\mathcal{R}}$. Alternatively, with probability $\xi_{\text{all}} = 1 - \xi_{\text{region}}$, they make an unconstrained choice from all available destinations j according to probabilities p_{ij} .

We supposed that each region of preference consists of destinations intersecting with a buffer of radius ρ around a subbasin centre (Figure 4). Each angler’s region of preference is fixed over time and chosen randomly. The probability $p_{i\mathcal{R}}$ that an angler from origin i has region of preference \mathcal{R} is proportional to how likely they would choose a destination in \mathcal{R} under the unconstrained strategy:

$$p_{i\mathcal{R}} = \frac{1}{\sum_{\tilde{\mathcal{R}} \in \mathfrak{R}} \sum_{j \in \tilde{\mathcal{R}}} p_{ij}} \sum_{j \in \mathcal{R}} p_{ij}. \quad (2)$$

Here, \mathfrak{R} is the set of all potential regions of preference. The probabilities $p_{ij|\mathcal{R}}$ are defined accordingly

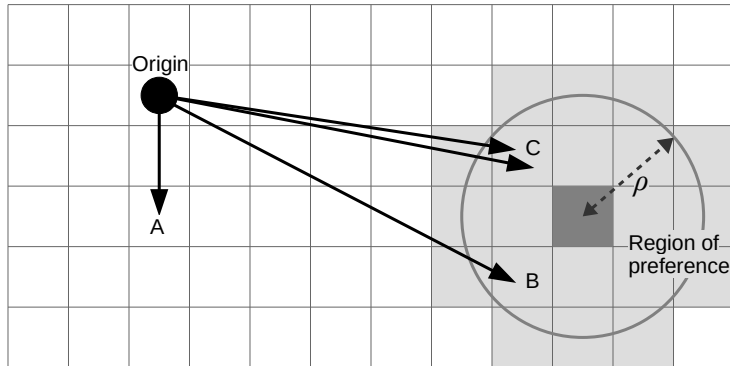


Figure 4: An example for a series of trips to destinations A , B , C , and again C in order (depicted as black arrows) for an angler with the region of preference drawn in grey. Each grid cell represents a destination. The region of preference contains all destinations intersecting with the buffer of radius ρ drawn around the centre of the destination coloured dark grey. The angler may choose any of the available destinations but often selects destinations within their region of preference. Furthermore, anglers may tend to revisit destinations on consecutive trips (e.g. destination C). Note that subbasins are not square grid cells in practice but can take any shape.

as

$$p_{ij|\mathcal{R}} = \frac{p_{ij}}{\sum_{\tilde{j} \in \mathcal{R}} p_{i\tilde{j}}}. \quad (3)$$

The assumptions above lead to a simplified model on an aggregate level. A random angler from origin i will choose destination j with probability

$$\xi_{\text{region}} \sum_{\mathcal{R} \in \mathfrak{R}} p_{i\mathcal{R}} p_{ij|\mathcal{R}} + \xi_{\text{all}} p_{ij} = p_{ij} \quad (4)$$

unless they revisit their previous destination. Note that they cannot revisit a destination on their first trip. The probability that they choose destination j on their second trip is therefore $(1 - \xi_{\text{same}})p_{ij} + \xi_{\text{same}}p_{ij} = p_{ij}$. By induction, the probability that a random angler from origin i chooses destination j is p_{ij} .

Since not all anglers in Alberta used the MyCatch app and app users may not have recorded all their trips, an additional submodel for the sampling process is needed to incorporate the data recorded via the app. We assumed that each angler decided randomly to install and use the app with probability ν_{app} , and that app users record a trip with probability ν_{record} .

2.3 Computing expected trip counts

Based on the model introduced above, the expected number of consecutive angler trips to destinations j_1 and j_2 can be computed as follows. Let n_i be the number of anglers residing at origin i . Then, the expected number of trips that anglers from origin i make during the study period is $n_i\mu_iT$. Now consider the probability that, for any pair of consecutive trips, j_1 is the destination of the first trip and j_2 is the destination of the second trip. Recall that anglers may either revisit their previous location, constrain their destination choice to their region of preference, or choose their destination freely. Hence, the mean number of consecutive trips by anglers from origin i to j_1 and j_2 during the study period is

$$\begin{aligned} \mu_{ij_1j_2} = & \underbrace{n_i\mu_iT}_{\text{expected trip count}} \left(\underbrace{\xi_{\text{same}}\delta_{j_1j_2}p_{ij_1}}_{\text{prob. to travel } j_1 \rightarrow j_2 = j_1 \text{ by choosing } j_1 \text{ and revisiting it without considering alternatives}} + \underbrace{(1 - \xi_{\text{same}})}_{\text{prob. to consider alternatives to previous dest. } j_1} \left(\underbrace{\xi_{\text{all}}^2}_{\text{prob. to travel } j_1 \rightarrow j_2 \text{ if both are chosen from all available sites}} \underbrace{p_{ij_1}p_{ij_2}}_{\text{prob. to travel } j_1 \rightarrow j_2 \text{ if both are chosen from all available sites}} \right. \right. \\ & \left. \left. + \xi_{\text{all}}\xi_{\text{region}} \left(\underbrace{p_{ij_1} \sum_{\mathcal{R}: j_2 \in \mathcal{R}} p_{i\mathcal{R}}p_{ij_2|\mathcal{R}}}_{\text{prob. to travel } j_1 \rightarrow j_2 \text{ if } j_1 \text{ is chosen from all available sites and } j_2 \text{ from a region of preference}} + \underbrace{p_{ij_2} \sum_{\mathcal{R}: j_1 \in \mathcal{R}} p_{i\mathcal{R}}p_{ij_1|\mathcal{R}}}_{\text{prob. to travel } j_1 \rightarrow j_2 \text{ if } j_1 \text{ is chosen from a region of preference and } j_2 \text{ from all available sites}} \right) + \xi_{\text{region}}^2 \sum_{\mathcal{R}: j_1, j_2 \in \mathcal{R}} p_{i\mathcal{R}}p_{ij_1|\mathcal{R}}p_{ij_2|\mathcal{R}} \right) \right) \end{aligned} \quad (5)$$

Here, $\delta_{j_1j_2}$ is 1 if $j_1 = j_2$ and 0 otherwise. The right hand side of equation (5) can be simplified to speed up computations, as we show in Appendix S2.

We computed the expected number $\mu_{j_1j_2}$ of consecutive trips to destinations j_1 and j_2 by summing $\mu_{ij_1j_2}$ over all origins i . To determine how many anglers access a destination j_2 after having visited a whirling-disease infested site, we furthermore summed the $\mu_{ij_1j_2}$ over all subbasins j_1 where the disease is present already. Based on these results, we also computed the number of these trips for each origin i .

2.4 Submodels for day suitability, angler activeness, and destination probabilities

The expected day suitability τ_t may change in weekly and seasonal cycles. We modelled these variations using the probability density function $f_{\text{vM}}(\cdot; \kappa, \theta)$ of the von Mises distribution, which is

a cyclic distribution resembling the normal distribution (Lee, 2010). The shape of the function is controlled via the two parameters θ , determining the location of the mode, and κ , determining how sharp the maximum is. We defined the expected suitability τ_t of day t as follows:

$$\tau_t = c_{\text{norm}} \underbrace{\left(c_{\text{week}} + f_{\text{vM}} \left(2\pi \frac{t \bmod 7}{7}; \theta_{\text{week}}, \kappa_{\text{week}} \right) \right)}_{\text{weekly variations}} \underbrace{\left(c_{\text{year}} + f_{\text{vM}} \left(2\pi \frac{t \bmod 365}{365}; \theta_{\text{year}}, \kappa_{\text{year}} \right) \right)}_{\text{yearly variations}}. \quad (6)$$

The constants c_{year} and c_{week} are parameters controlling the amplitude and vertical shift of the weekly and seasonal cycles; the constant c_{norm} is chosen so that $\frac{1}{T} \sum_t \tau_t = 1$. If the study period includes leapyears, τ_t must be adjusted accordingly.

As the 2104 trips in our dataset did not suffice to estimate the choice probabilities p_{ij} for all 180,000 pairs of localities and subbasins directly, we estimated μ_i and p_{ij} based on covariates on the origins and destinations. To that end, we applied the framework of gravity models. Gravity models estimate the mean number of trips between each origin and destination as a product of (1) the *repulsiveness* of the origin, proportional to the number of outbound trips; (2) the *attractiveness* of the destination, proportional to the number of inbound trips; and (3) a decaying function of the distance between origin and destination. Repulsiveness and attractiveness are typically functions of covariates characterizing the origins and destinations. In our model, the expected outbound traffic of origin i is given by the product $n_i \mu_i$ of angler count and activeness, and the expected traffic between origin i and destination j is $n_i \mu_i p_{ij}$. Therefore, the repulsiveness of origin i corresponds to the product $n_i \mu_i$, whereas the product of distance decay function and attractiveness defines the choice probabilities p_{ij} . Let d_{ij} be the linear distance between origin i and destination j , and let a_j be the attractiveness of destination j , measuring both the quantity and quality of fishing opportunities. Then,

$$p_{ij} = \frac{a_j D(d_{ij})}{\sum_{\tilde{j}} a_{\tilde{j}} D(d_{i\tilde{j}})}, \quad (7)$$

with the distance decay function D , which we define as

$$D(d_{ij}) = \frac{d_0^{\text{distance}}}{d_0^{\text{distance}} + d_{ij}^{\text{distance}}}. \quad (8)$$

The parameter d_0 is the half saturation constant, given as the distance at which $D(d_{ij}) = \frac{1}{2}$.

To define an appropriate function to compute μ_i and a_j based on the covariates, we categorized the covariates into groups \mathcal{X} (Table 1), each accounting for a different component that is necessary for high angler traffic between an origin and a destination (cf. Fischer *et al.*, 2020). For each origin or destination k , we assigned the score $(\beta_{\mathbf{x}}x_k)^{\gamma_{\mathbf{x}}}$ to each covariate $\mathbf{x} \in \mathcal{X}$, where x_k is the component of \mathbf{x} corresponding to k and the parameters $\beta_{\mathbf{x}}$ and $\gamma_{\mathbf{x}}$ describe the impact of \mathbf{x} . We then added these individual scores to obtain a score for each group \mathcal{X} , so that a high score for *one* covariate suffices to make the group’s score large. Finally, we multiplied the scores for the different groups, making a high score for *all* components necessary to boost the number of angler trips. With scaling constant c , we set

$$\mu_i = c \prod_{\substack{\text{origin covariate} \\ \text{groups } \mathcal{X}}} \left(1 + \sum_{\mathbf{x} \in \mathcal{X}} (\beta_{\mathbf{x}}x_i)^{\gamma_{\mathbf{x}}} \right), \quad (9)$$

$$a_j = \prod_{\substack{\text{destination covariate} \\ \text{groups } \mathcal{X}}} \left(1 + \sum_{\mathbf{x} \in \mathcal{X}} (\beta_{\mathbf{x}}x_j)^{\gamma_{\mathbf{x}}} \right), \quad (10)$$

where the *origin* and *destination covariate groups* are the locality and subbasin groups in Table 1.

2.5 Fitting the model

We fitted the model via maximizing the likelihood associated with the recorded app data. However, fitting the complete model all at once is computationally costly due to the complicated form of the likelihood function and the large number of parameters. Therefore, we eliminated parameters by summing over certain quantities to obtain submodels with simpler likelihood functions. Furthermore, we made approximations via independence assumptions, disregarding the identity of anglers in some fitting stages (see below). Since most trips are made by independent anglers, our parameter estimates remain valid despite these simplifications (Varin, 2008).

We fitted the model in three steps: first, we considered the submodel for the day suitability ε_t ; second, we estimated the angler activeness μ_i and the destination choice probabilities p_{ij} ; and third, we estimated the parameters ξ_{same} , ξ_{region} , ξ_{all} , ν_{app} , ν_{record} , and ρ modelling anglers’ tendencies to constrain their trip choices and to record trips. Below, we briefly explain each of these steps; more details can be found in Appendix S3. In each of the steps, we exploited that (1) a Poisson random

variable with a gamma distributed mean is negative binomially distributed and that (2) the mixture of a negative binomial and a binomial distribution remains negative binomially distributed (Villa & Escobar, 2006).

2.5.1 Day suitability

We estimated the expected day suitability τ_t by fitting the distribution of the total number N_t of recorded angler trips on day t to the data. According to our model, N_t is negative binomially distributed with dispersion parameter $\frac{\alpha}{\tau_t}$ and mean $\nu_{\text{record}}\tau_t \sum_i \tilde{n}_i \mu_i$, where \tilde{n}_i is the number of app users in locality i . As \tilde{n}_i is a random variable itself and constant over the study period, it is not straightforward to derive the exact distribution of N_t . However, since N_t describes the aggregate trip counts of many anglers, who rarely make more than one trip per day, it is reasonable to consider trips as mutually independent on each day. Then, the distribution of N_t is negative binomially distributed with dispersion $\frac{\alpha}{\tau_t}$ and mean $\tau_t \bar{\mu}$, where $\bar{\mu} = \nu_{\text{app}}\nu_{\text{record}} \sum_i n_i \mu_i$. Hence, by fitting the distribution of N_t , we obtained estimates for the parameters α , $\bar{\mu}$, and those controlling the shape of τ_t . See Appendix S3.1 for further details.

2.5.2 Angler activeness and destination choice probabilities

To estimate the angler activeness values μ_i and the destination choice probabilities p_{ij} , we considered the trip counts N_{ijt} for origin-destination pairs (i, j) and days t . We fitted the joint distribution of the N_{ijt} to our data for all origin-destination pairs and days of the study period. With the independence approximation from the previous section, each N_{ijt} follows a negative binomial distribution with dispersion parameter $\frac{\alpha}{\tau_t}$ and mean $\nu_{\text{app}}\nu_{\text{record}}\tau_t n_i \mu_i p_{ij}$. To improve the computational performance, we also considered the trips from different localities as mutually independent. The values τ_t were known from the previous fitting stage. By fitting N_{ijt} to the observed values, we obtained estimates for the parameters of μ_i and p_{ij} . The scaling constant c and the probabilities ν_{app} and ν_{record} are not identifiable in this fitting stage, and we replaced them with a parameter $C = \nu_{\text{app}}\nu_{\text{record}}c$ here. Refer to Appendix S3.2 for a method to compute the likelihood efficiently.

2.5.3 Remaining parameters

To fit the choice parameters ξ_{same} , ξ_{region} , ξ_{all} , ν_{app} , and ν_{record} , we considered each angler and their trips individually. First, we determined the likelihood for the temporal sequence of their trips. Then we computed the likelihood for their destination choices given the timing of the trips. Because the destination choices for consecutive trips are not independent and we need to consider unknown numbers of intermediate unrecorded trips, the likelihood function has a complicated form involving convolutions and special functions. Nonetheless, it can be computed numerically with reasonable effort if partial intermediate results are reused where possible. We refer the reader to Appendix S3.3 for details. Dependencies between trips of *different* anglers were disregarded at this stage so as to facilitate efficient computation.

To fit the radius ρ of the inscribed circle of anglers' regions of preferences, we conducted a grid search with steps of 1 km in the interval between 10 km and 80 km. For each considered value of ρ , we maximized the likelihood with respect to the remaining parameters; finally, we chose the radius leading to the maximal likelihood. We conducted a grid search, because the regions of preference are discrete entities, making gradient descent methods inapplicable to fit ρ .

2.5.4 Optimization methods and model selection

We used a combination of multiple optimization algorithms to maximize the likelihood. We applied the differential evolution algorithm (Storn & Price, 1997) for a global search of the parameter space, and improved upon the results via gradient-based search algorithms (Kraft, 1988; Byrd *et al.*, 1995; Nocedal & Wright, 2006). Details can be found in Appendix S4. We implemented the model in the programming language Python (version 3.7) along with the Scipy libraries (Jones *et al.*, 2001).

To decide which covariates and parameters should be included in the model without overfitting, we used the information criterion by Akaike (1974) (AIC). This metric is particularly suitable if the modelling goal is prediction (Ghosh & Samanta, 2001). When fitting the day suitability function τ_t , we considered simplified models with the parameters c_{week} , c_{year} , κ_{week} , and κ_{year} , (equation (6)) set to 0, respectively. For the angler activeness μ_i and destination choice probabilities p_{ij} , we considered models with any combination of the parameters $\beta_{\mathbf{x}}$ and $\gamma_{\mathbf{x}}$ (equations (9)-(10)) set to zero. Only for covariates \mathbf{x} that had 0-values for some origins or destinations, we tested models with $\gamma_{\mathbf{x}} = 1$

instead. We furthermore tested models without the parameter d_0 (equation (8)). We searched for the model with the minimal AIC value by using a branch and bound algorithm (Appendix S4.2). This allowed us to find the optimal model without having to consider all potential candidates.

Note that we made approximations via independence assumptions, which violate the underlying assumptions of AIC. Hence, the metric may tend to favour overfitting models. We therefore chose the simplest model among those with AIC values less than 10 units higher than the minimal AIC. Models whose AIC value is more than 10 units higher than the minimal AIC may have little empirical support (Burnham & Anderson, 2004).

2.5.5 Model evaluation

We evaluated the trustworthiness of our parameter estimates by computing confidence intervals using a method based on the profile likelihood (Fischer & Lewis, 2021). Note that since we did not evaluate the joint model all at once and made approximations via independence assumptions, the true confidence intervals may be larger. Nonetheless, the approximate confidence intervals are suited to detect estimability issues and problems arising from multicollinearity of covariates.

To validate the submodel for angler traffic between localities and subbasins, we randomly split the app data into a training (fitting) and a testing (validation) dataset, each containing observations for half of the anglers, respectively. Note that a random split is in line with our purpose of evaluating the model accuracy in predicting unreported trips, and hence, a temporal split used for evaluating the model accuracy in making future predictions is not needed (Ramazi *et al.*, 2021b). We fitted our model to the training data and computed the mean yearly number of recorded angler trips for each origin, destination, and origin-destination pair. Then we plotted the predicted values against the observed values.

The purpose of the submodel for locality-to-subbasin traffic was to fill data gaps stemming from the limited number of angler trips in our dataset. To ensure that the model is suited to fill these gaps without introducing additional error, we computed the mean absolute errors between the submodel's results and the observations from the testing data. We then compared the resulting values with those obtained by using direct estimates from the training data without an additional model.

Our model yields absolute estimates of angler traffic based on voluntarily reported trip data

without using a priori information on how many trips anglers actually made. To assess the accuracy of our estimates of the trip frequency, we compared the number of days anglers go fishing per year as per our model (see Appendix S5) with empirical data collected in a mail-out survey by the Department of Fisheries and Oceans Canada in 2016 (DFO, 2019).

To facilitate a qualitative comparison of our model’s accuracy with predictions from similar studies, we computed Nagelkerke’s pseudo- R^2 (Nagelkerke, 1991). This measure indicates how well the model performs in comparison to a non-informative null model. In contrast to the classical R^2 , Nagelkerke’s pseudo- R^2 can be applied even if the data are not assumed to be normally distributed with identical standard deviations. We computed pseudo- R^2 values for each model stage: the day suitability model; the joint day suitability, angler activeness and destination choice model; and the complete model with all submodels. As null models, we used negative binomial distributions treating all days, localities, and subbasins similarly. The parameters ξ_{same} and ξ_{region} capturing anglers’ local preferences were set to zero.

3 Results

The selected day suitability model contained all considered parameters (Table 2). The traffic was estimated highest on Saturdays and to peak on July 14. The rates of fishing trips during the weekly peak was estimated to be 2.27 times higher than on the weekly low; yearly cycles changed the expected traffic rate by up to factor 6.6. The confidence intervals were relatively narrow for most of the parameters; only the shape parameter for the weekly cycles had a large upper confidence interval bound. The temporal distribution of trips and the expected trip rates estimated by the model are displayed in Figure 5.

The angler activeness and destination choice model with the least number of parameters and $\Delta\text{AIC} \leq 10$ included 15 parameters (Table 3; $\Delta\text{AIC} = 1.5$). The model with minimal AIC included the number of website visits as an additional covariate. The selected model uses localities’ population counts and the mean income numbers to estimate angler activeness. The angler activeness varied by up to factor 4.5 among localities. For a locality with median characteristics, a population increase of 1000 increases angler activeness by 6%, and a mean income increase by CAD 1000 increases activeness by 2%.

Parameter	Explanation	Estimate	Confidence Interval	
α	Dispersion parameter	0.33	0.25	0.42
$\bar{\mu}$	Mean total recorded trips per day	2.56	1.52	4.34
c_{week}	Week addition constant	0.45	0.24	0.7
θ_{week}	Week location constant	5.64	5.5	5.8
κ_{week}	Week shape constant	2.87	1.36	∞
c_{year}	Year addition constant	0.12	0.1	0.15
θ_{year}	Year location constant	3.35	3.29	3.42
κ_{year}	Year shape constant	7.4	6.53	8.29

Table 2: Parameters and estimates along with approximate 95% confidence intervals after fitting the model to the daily trip counts.

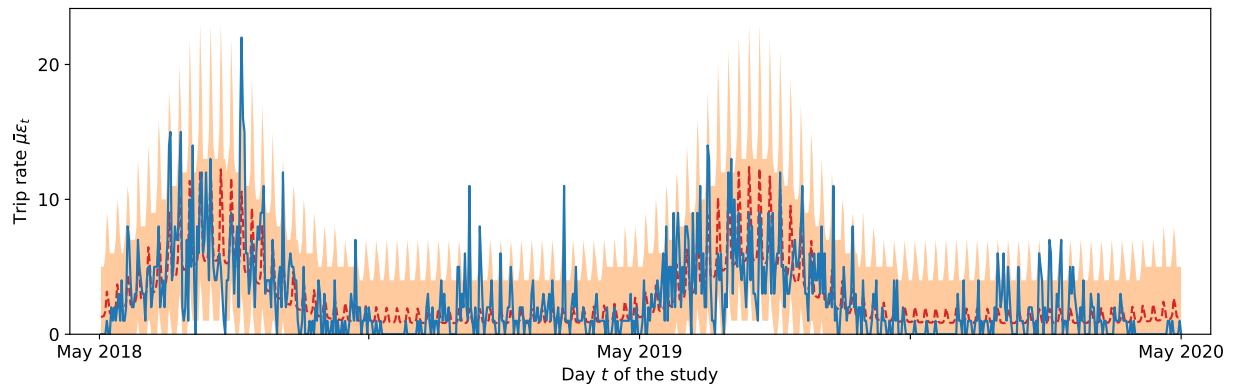


Figure 5: Observed and modelled trip rates for each day of the study period. The observed number of trips N_t is drawn as solid blue line, the predicted mean of N_t as dashed red line, and the predicted 95% confidence range as light red area.

The localities from which anglers make the most consecutive trips between infested and uninfested subbasins were the population centres Calgary and Edmonton. Setting the trip count into relation with the number of registered anglers, Calgary, located in direct proximity to the infested area, had higher relevant traffic with 2.86 high-risk trips per registered angler and year as compared to 0.65 for Edmonton. Considering all inhabitants, rural municipalities had higher relative trip counts: the 100 localities with the most high-risk trips per inhabitant had less than 8000 inhabitants.

The subbasin attractiveness was estimated based on the perimeter of the waterbodies in the subbasins, the surface area of the waterbodies with confirmed species, the number of campgrounds, and the website species upvotes. The attractiveness values varied greatly among subbasins, by up

Parameter	Explanation	Estimate	Confidence Interval	
α	Dispersion parameter	6.99	4.91	9.59
C	Scaling constant for the mean daily number of recorded trips	$1 \cdot 10^{-9}$	$3.51 \cdot 10^{-11}$	$5.12 \cdot 10^{-8}$
δ_0	Distance of half choice-probability decay [km]	28.74	22.02	35.91
γ_{distance}	Distance exponent	2.09	1.97	2.22
$\beta_{\text{population}}$	City population factor [$1/10^3$]	$6.95 \cdot 10^{29}$	$4.29 \cdot 10^{29}$	$1.23 \cdot 10^{30}$
$\gamma_{\text{population}}$	City population exponent	0.14	0.09	0.16
$\beta_{\text{mean income}}$	Mean income factor [$1/(10^3 \text{CAD})$]	909.1	11.61	$2.3 \cdot 10^6$
$\gamma_{\text{mean income}}$	Mean income exponent (not included in the model)	1	–	–
$\beta_{\text{perimeter}}$	Water perimeter factor [$1/(10^3 \text{km})$]	0.82	0.76	0.94
$\gamma_{\text{perimeter}}$	Water perimeter exponent	6.76	3.89	9.62
$\beta_{\text{area confirmed}}$	Water area confirmed factor [$1/(10^3 \text{km}^2)$]	38.95	9.25	305.8
$\gamma_{\text{area confirmed}}$	Water area confirmed exponent	0.4	0.24	0.67
$\beta_{\text{campground}}$	Campground factor [1]	0.25	0.12	0.62
$\gamma_{\text{campground}}$	Campground exponent	1	0.65	1.46
$\beta_{\text{species vote}}$	Species vote factor [1]	2.8	1	8.4
$\gamma_{\text{species vote}}$	Species vote exponent	0.57	0.5	0.65

Table 3: Parameters and estimates along with approximate 95% confidence intervals after fitting the model for angler activeness and destination choice. Note that though we report all parameters on the original scale, we worked with log-transformed parameters internally to avoid numerical errors due to extreme parameter values.

to factor 1179. For a subbasin with median characteristics, an increase in the total waterbody perimeter by 500 km increased attractiveness by 8.7%, whereas an increase of 1000 km increased attractiveness by factor 3. If the total area of waterbodies with confirmed species were increased by 10 km^2 , attractiveness would rise by 69%. An additional campground increased attractiveness by 20%, and an additional positive species vote by 180%. The traffic between localities and subbasins decreased in square order of their distance; i.e., a subbasin twice as far as a similar subbasin was only 25% as likely to be chosen as fishing destination.

The estimates for the remaining choice parameter are displayed in Table 4. The fraction of anglers using the app was estimated to be 0.22%, and the estimated probability that app users report a trip was 0.05. The dispersion parameter, modelling the impact of stochastic events on anglers' daily trip rates was estimated 11.8. The model predicts that on 64% of their trips, anglers

Parameter	Explanation	Estimate	Confidence Interval	
α	Dispersion parameter	11.81	8.65	15.6
ξ_{same}	Probability to revisit the previous destination	0.64	0.53	0.79
ξ_{region}	Probability to constrain the destination choice to the region of preference	0.54	0.5	0.59
ν_{app}	Probability to use the app	0.0022	0.0021	0.0023
ν_{record}	Probability to record a trip	0.052	0.022	0.104

Table 4: Parameters and estimates along with approximate 95% confidence intervals after fitting the model for the individual angler choices

revisit their last destination. They choose a destination in their region of preference in 54% of their trips and choose the destinations for the remaining 46% trips from all over Alberta. The estimated radius ρ for the inscribed circle of regions of preference was 31 km. This translates to a mean radius of 54.7 km for the regions of preference. The parameter confidence intervals were relatively narrow except for the probability that app users report a trip (Table 4).

Angler trips were estimated to be strongest between subbasins located close to metropolitan areas, with estimates up to 22.3 thousand (95% confidence interval $[14.5 \cdot 10^3, 32.6 \cdot 10^3]$) directly consecutive angler trips per year (Figure 6a). The subbasin most at risk of receiving anglers infested with whirling disease propagules were those located close to larger cities and in proximity to the already infested area (Figure 6b). The subbasin with the highest inflow of high-risk trips was estimated to receive 27.7 thousand ($[18.1 \cdot 10^3, 40.3 \cdot 10^3]$) such trips per year. The estimated mean number of fishing days per angler and year was 20.5 ($[12.5, 34.1]$) as per our model. For comparison, the corresponding estimate from a 2016 mail-out survey was 18 (standard deviation between 0.9 and 2.7) (DFO, 2019).

The pseudo- R^2 values of the model components decreased as more complexity was added. The submodel for the day suitability achieved a pseudo- R^2 of 0.47. Adding the component for the origin-dependent trip rates and the destination choice probabilities yielded a value 0.35. Predicted and observed values for this model component are depicted in Figure 7. The joint model including the remaining choice parameters had a pseudo- R^2 of 0.26.

The submodel for the traffic between origins and destinations estimated the outflow from origins

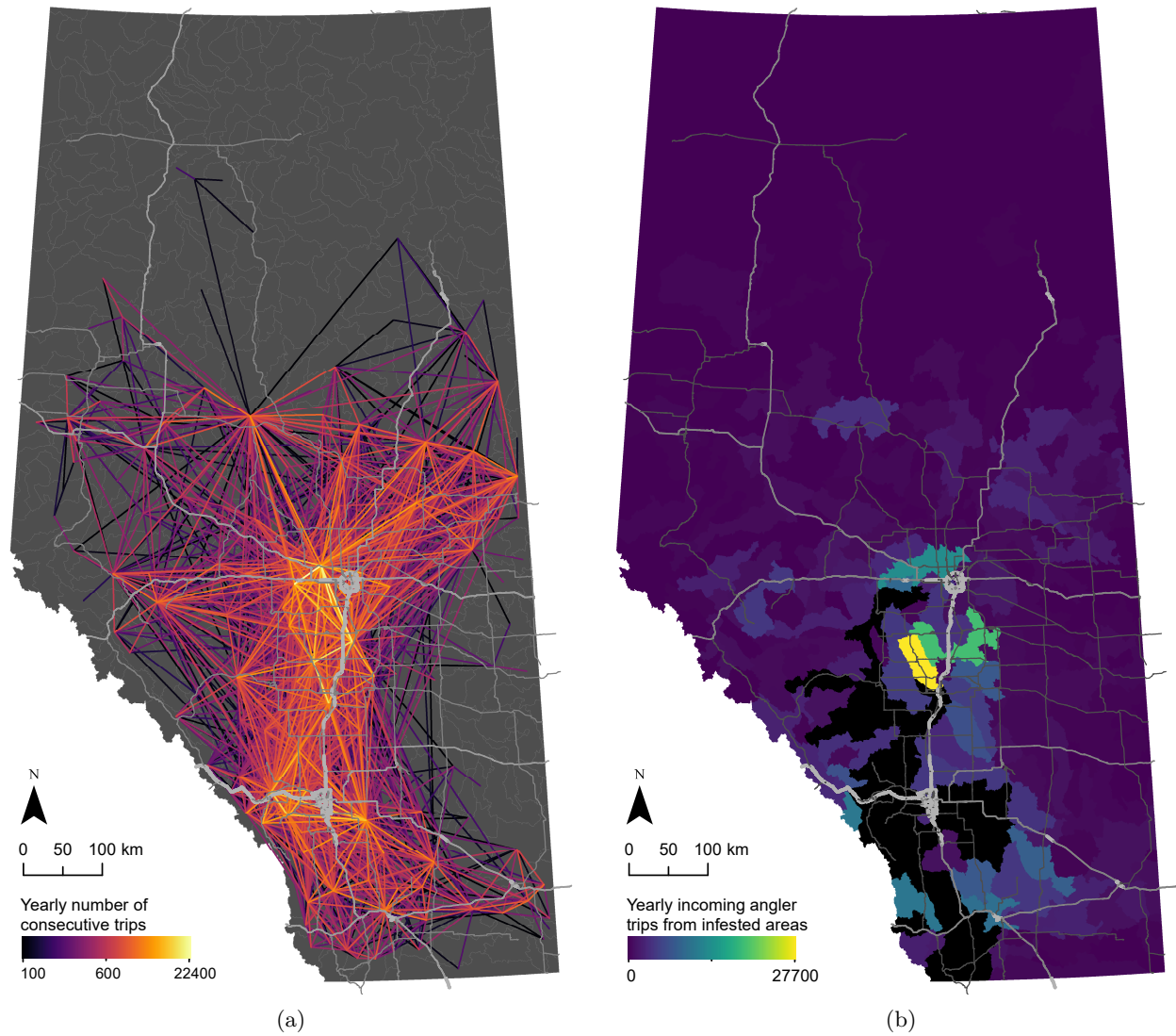


Figure 6: (a) Number of consecutive trips to subbasin pairs and (b) total number of incoming trips by potentially infested anglers. In (a) only subbasin pairs with more than 100 trips per year are shown. In (b) black colours depict subbasins that are already infested (March 2020).

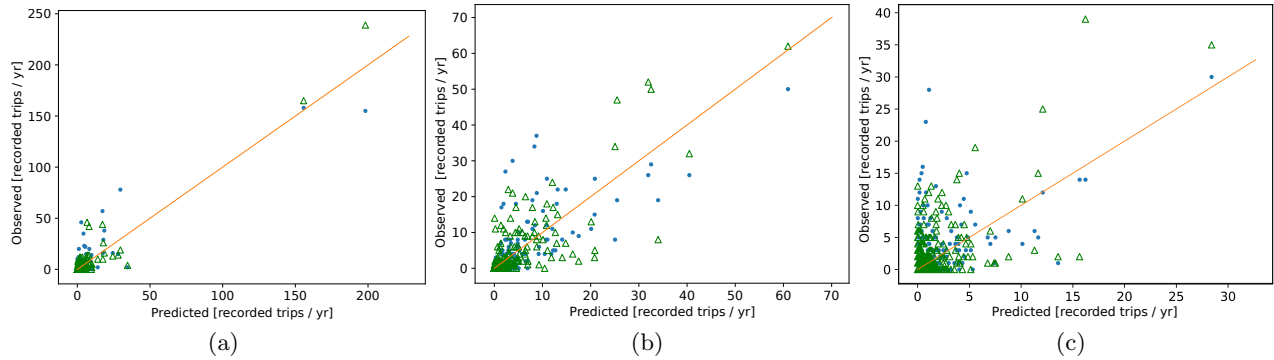


Figure 7: Predicted and observed mean values of yearly recorded angler trips (a) by origin locality, (b) by destination subbasin, and (c) by locality-subbasin pair. The values used to fit the model are depicted as solid blue circles; the values computed from the independent fitting dataset are drawn as hollow green triangles. The orange line indicates where predictions and observations would coincide.

with a mean error of 1.48, the inflow to destinations with a mean error of 1.6 and the traffic between individual pairs with a mean error of 0.0073. The corresponding values obtained by using the data directly were 1.83, 1.81, and 0.0074. That is, applying the model did not increase the error.

4 Discussion

Mobile apps exist for a variety of outdoor activities (e.g. birding, hiking and fishing) that could be related to the spread of animal diseases and invasive species. These apps can yield highly detailed individual-specific, spatially and temporally representative data and provide valuable insights into the traffic of anthropogenic vectors of invasive species and pathogens (Papenfuss *et al.*, 2015; Venturelli *et al.*, 2017). However, though the datasets collected via mobile apps can be large, they often cover only a small fraction of all trips of potential vectors, making direct estimates via the data’s empirical distribution error-prone. Our results indicate that modelling approaches can reduce this issue and provide additional insights into the mechanisms behind vector movement.

Conversely, models can profit strongly from the new data source. Though mail-out or online surveys could collect the same data as apps in principle, our modelling approach based on app data has the following advantages:

(1) Increased accuracy. Apps can be downloaded by users from different geographical areas, and data may be collected over extended time periods. Therefore, inference from app data is generally

less sensitive to local and temporal peculiarities, and modellers can identify and account for the sources of spatial and temporal heterogeneity. This makes the estimates more accurate, especially when results are extrapolated into the future or to larger geographical scales. Furthermore, the temporal fingerprint of app data records permits a longitudinal study design. By considering the day-to-day variations of the data, the unexplained recurring stochasticity in individual decisions can be distinguished from systemic errors due to misspecified models. Without this distinction (e.g. Drake & Mandrak, 2010; Muirhead *et al.*, 2011; Muirhead & MacIsaac, 2011), residuals would be solely attributed to the stochasticity in the individuals' decisions, and the dispersion parameter would be overestimated (Fischer *et al.*, 2020). Then, low-traffic angler flows gain an inordinate weight when the model is fitted to observations, resulting in decreased model accuracy (see Appendix S6).

(2) Estimates account for reduced vector mobility due to individual preferences. Accounting for anglers' individual preferences allowed us to estimate the frequency at which they switch destinations, potentially transporting propagules. We found that in 64% of their trips, anglers revisit their previous destination and hence do not spread invasive species and pathogens to new areas. Furthermore, anglers tend to choose half of their fishing destinations from spatially contained areas. This suggests that models disregarding the correlations within anglers' destination choices (e.g. Bossenbroek *et al.*, 2001; Leung *et al.*, 2004) are prone to overestimating traffic between distant destinations.

(3) Absolute estimates of vector traffic can be obtained without additional survey data. It is difficult to obtain absolute traffic estimates from survey or app data without knowing which fraction of trips surveyed individuals or app users report. However, by considering anglers' tendency to revisit previous destinations, we were able to infer this missing information. If an angler does not record all their trips, the probability that the next trip they record has the same destination as their previously recorded trip decays with time, because they may make additional unrecorded trips to other destinations in the mean time. The slope at which the fraction of consecutively recorded trips with same destinations decays with the intermediate time depends on the trip recording probability. This makes it possible to infer this information from the data.

Absolute estimates of traffic enable modellers to link traffic to invasion or infection success. This link is needed to predict the spread of a disease or invasive species (Lewis *et al.*, 2016). Though invasion success can be estimated based on relative traffic estimates if historical invasion data are available for the studied area (Leung *et al.*, 2004; Muirhead *et al.*, 2006; Potapov *et al.*, 2011), these estimates will remain site-specific unless the scaling of the traffic is known or the same traffic model is at the other site. Transferring a traffic model to a new site requires that similar data are available at the new site and that vectors behave the same. Absolute traffic estimates allow modellers to estimate the establishment success per individual vector and to transfer such information to or from other study areas.

Validity of the estimates

Exploiting the connection between reported destinations and the completeness of the data, we estimated how many days an average angler goes fishing in Alberta per year. Our estimate for this quantity agreed with an independent estimate, differing only by about one standard deviation of the independent estimate. This suggests that our approach estimates the overall angler trip frequency accurately and hence can be used to obtain absolute traffic estimates even if the fraction of reported trips is unknown. Note, however, that the confidence interval for our estimate was relatively large and had an upper bound 60% higher than the estimated value. Hence, additional surveys determining the total trip count – and thereby the fraction of reported trips – remain worthwhile to reduce model uncertainty. We refrained from incorporating this additional information, because our estimate of the total trip counts was already in agreement with the independent estimate.

The predicted vs. observed analysis of the submodel for angler activeness and destination choice probabilities indicated a reasonable estimation accuracy. Comparison with the raw data showed that the model extrapolates the limited available data to all origin-destination pairs without introducing additional error – the model did even slightly better than the direct estimates. This is due to the stochasticity inherent in the system and the limited number of available trip records.

The pseudo- R^2 values we computed for different model components decreased as more complexity was added. This is expected, because the level of detail of the validation data increased as additional model components were considered. The differing level of detail makes it difficult to compare our pseudo- R^2 values to similar metrics obtained in studies with less rich data sources (e.g.

Drake & Mandrak, 2010; Chivers & Leung, 2012). Nonetheless, the pseudo- R^2 value we reported may be a helpful benchmark for future studies on a similar system.

Management implications

Our approach facilitates management in three ways: (1) it provides location-specific risk proxies; (2) it shows which locations are best connected and might thus be potential hubs for secondary infections; and (3) it helps to identify the origins of the agents most at risk spreading the disease. While risk estimates facilitate early detection and rapid response to new infections, the latter two points help targeting management actions to the subbasins and localities where they are most effective.

(1) Risk proxies The subbasins with the highest propagule inflow were those encompassing extended water areas with confirmed fish presence and located close by a population centre in proximity of an infected subbasin. Our results indicate that anglers show a strong preference for fishing destinations near their homes, which also agrees with earlier studies (Drake & Mandrak, 2010; Papenfuss *et al.*, 2015; Fischer *et al.*, 2020). Both the inscribed radius of the regions of preference and the distance at which traffic decays by half were at about 30 km, suggesting this as main spatial scale of angler traffic. Besides water area and fish species confirmations, the number of campgrounds was another useful indicator of attractiveness, probably because they are typically built in scenic areas attractive to outdoor tourists.

The total waterbody circumference (i.e., shoreline) was positively connected with angler traffic as well, but the best-AIC model did not incorporate this covariate in conjunction with fish presence data, potentially due to incomplete species data in smaller rivers. Interestingly, the number of visits of waterbody-specific websites was not a worthwhile additional predictor for attractiveness – perhaps because this number is also affected by the waterbodies’ proximity to angler origins and their repulsiveness.

(2) Potential hubs Uninfected subbasins with strong connections to other uninfected subbasins might become significant hubs for secondary infections. This makes these well-connected subbasins a primary target for surveillance and rapid response measures. In our model, these subbasins have

similar characteristics to those receiving most high-risk trips (see above) except for being located farther away from present infections.

(3) Most relevant angler origins Education and outreach measures may be applied with different intensity in different localities. According to our results, maximal high-risk trip counts per inhabitant are found in rural areas, where the density of anglers per inhabitant is higher there than in cities. Hence, general outreach may be most effective in rural areas close to the edge of the infested area. In contrast, the number of high-risk trips per angler was also high in cities, making cities close to the infected area good soil for outreach measures specifically targeting anglers. Outreach may be cheaper and hence more cost-effective in cities than in rural areas.

Limitations and potential extensions

Voluntarily reported data such as app data can be prone to a variety of biases ranging from demographic bias to avidity bias (Venturelli *et al.*, 2017). For example, app usage may be higher among the young population from urbanized areas, and active sport fishers may use the app more frequently. As a result, certain demographic groups may be underrepresented, and highly active app users may influence the estimates disproportionately. This can lead to biased and over-confident results.

For the data from the MyCatch app used in this study, no spatial bias was detected (Johnston *et al.*, 2021). This increases the credibility of our results. Nonetheless, some potential sources of bias remain, and other datasets may suffer from stronger bias. This issue could be addressed with additional data. If demographic and socioeconomic data are collected along with the other app data, these covariates could be directly incorporated into the model. If an independent sample with these data is available, it can be used to weigh the observations differently (Chen *et al.*, 2020).

Our model uses socioeconomic covariates to estimate the activeness of anglers at different localities. Though incorporating population counts and the mean income in localities improved the model fit significantly, angler activeness is unlikely to be uniform within localities. Since there is no obvious mechanistic justification for the dependency of angler activeness on the covariates we used, we emphasize the phenomenological nature of the model and refrain from further analysis of the underlying mechanisms.

We also assume that the individual preferences of individuals do not change with time. This assumption may be inaccurate if extended time periods are considered, and individuals may change both their region of preference and their home place. As a result, the connectivity of close-by locations in directly consecutive trips might be underestimated. This issue could be addressed by splitting the dataset into subsets for different time periods and to treat them as independent replicates of one another.

By fitting model components in separate steps, we obtained multiple estimates for the dispersion parameter α . This indicates that some sources of stochasticity, such as weather, act on small scales only and have a reduced impact on an aggregate level. This is a common effect seen in ecological models (Dungan *et al.*, 2002) and difficult to resolve without ignoring spatial correlations completely or strongly increasing the model’s complexity. However, since the estimates for the other parameters were insensitive to moderate variations of the dispersion parameter (Appendix S7), our estimates for the mean angler traffic remain valid despite the scale-dependency of the dispersion parameter.

Noting that propagules may be washed out at any site visited by anglers, we concentrated on estimating the number of consecutive fishing trips to distinct subbasins. This is in line with existing studies on invasive species transport (Bossenbroek *et al.*, 2001; Leung *et al.*, 2004; Potapov *et al.*, 2011; Muirhead & MacIsaac, 2011). An alternative approach is to consider all trips that anglers make within the time frame propagules may survive (Papenfuss *et al.*, 2015). Note, however, that we assumed that anglers choose their destinations independently of the past unless they revisit their previous destination. Therefore, the number of higher-order trips between two subbasins equals the count of directly consecutive trips unless a constrained time frame is considered. Thus, incorporating higher-order trips comes down to determining a sensible time scale for propagule decay.

We focused on intra-provincial angler traffic, but our model could be extended to also consider non-resident anglers visiting the province on vacation trips. Within our model framework, such anglers could be added to the populations of the localities where they reside temporally. However, in Alberta, non-resident anglers are responsible for only 2.6% of the angler traffic (measured in yearly fishing days) (DFO, 2019), which is below the error margin of our estimates.

Alternative approaches

Our model’s complexity is driven by the challenges stemming from missing trip records in app data. If complete trip records were available, a phenomenological gravity model for the connectedness of destinations (e.g. [Potapov *et al.*, 2010](#); [Muirhead & MacIsaac, 2011](#); [Chivers & Leung, 2012](#)) could be constructed directly. However, complete trip records are often difficult to obtain without strong simplifying assumptions, such as that vectors have visited all destinations they reported with the same frequency ([Potapov *et al.*, 2010](#)).

If data on the temporal progression of the disease or invasion are available, the connectedness between destinations could also be inferred based on the observed infestation dynamics ([Bossenbroek *et al.*, 2001](#); [Leung *et al.*, 2004](#)). However, the resulting traffic estimates can typically not be validated due to the lack of data. Besides, this approach makes it necessary that an establishment model exists that accounts for on-site conditions affecting establishment success.

5 Conclusion

The increasingly widespread use of mobile apps by anglers, hikers, campers, and other potential vectors of invasive species and pathogens opens new opportunities for research and management. To exploit the full potential of this new data source, models accounting for spatial, temporal, and individual heterogeneity are needed. The presented model demonstrates the wealth of information that can be gained from app data, including (1) temporally explicit estimates of vector traffic between cities and waterbodies, (2) estimates of how often vectors choose new trip destinations, potentially carrying propagules to other places, and (3) the spatial scale at which individual local preferences play a major role in vectors’ decisions. Our results suggest that ignoring individual-specific components in vectors’ decision making can bias estimates by underestimating local traffic and overestimating long-distance traffic. We furthermore showed that incorporating vectors’ tendency to revisit past locations can bridge the common data gap arising from incomplete trip records reported by app users.

Acknowledgements

All authors are thankful for the funding received from Alberta Environment and Parks. In addition, PR and MAL thankfully acknowledge an NSERC Discovery Grant and MAL also gratefully acknowledges a Canada Research Chair. All authors would like to thank the anglers who voluntarily provided data via the MyCatch app and the Anglers' Atlas website. Furthermore, the authors thank the Goldstream Publishing staff, who helped prepare the data for the analysis as well as the members of the Lewis Research Group, who contributed through helpful feedback and discussions.

Conflict of interest

Sean Simmons is founder and president at Angler's Atlas and MyCatch. The authors declare no conflict of interest.

Author contributions

Pouria Ramazi, Sean Simmons, Mark S. Poesch, and Mark A. Lewis conceived the project. Sean Simmons collected and prepared the app data and the website data. All authors contributed to the methods; Samuel M. Fischer finalized and implemented the model. Samuel M. Fischer and Pouria Ramazi led the writing of the manuscript. All authors contributed critically to the drafts and gave final approval for publication.

Data Availability

The sources of the data used in this study are listed below. The code used in this study can be found at github.com/vemomoto/indspevemo. The compiled dataset used in this study is available via the Dryad Digital Repository doi.org/10.5061/dryad.6m905qg3j (Fischer et al., 2022).

Data Sources

Data	Source	URL
Angler App Data	Goldstream Publishing	The raw data are not available online. A compilation of the data used as input for the model will be made available along with the article.
Website Visit Data		
Species Vote Data		
Waterbody GIS Data		
Subbasin GIS Data	Government of Alberta (Alberta Environment and Parks)	Original URL (not available anymore): maps.alberta.ca/genesis/rest/services/Hydrologic_Unit_Code.Watersheds_of_Alberta Potential alternative data source: geospatial.alberta.ca
Locality GIS Data	Open Street Map	www.openstreetmap.org
Campground GIS Data	USCAmpgrounds	www.uscampgrounds.info
Angler License Count Data	Government of Alberta (Alberta Environment and Parks)	Retrieved through a standard data request from the Fish and Wildlife Management Information System www.alberta.ca/access-fwmis-data.aspx
Population Count Data	Government of Alberta	open.alberta.ca/opendata/alberta-municipal-affairs-population-list
Population Income Data	Government of Alberta	open.alberta.ca/dataset/labour-income-profile-for-all-forward-station-areas-city-totals-and-rural-postal-codes-canada-2013

References

- Akaike, H. (1974) A new look at the statistical model identification. *IEEE Transactions on Automatic Control*, **19**, 716–723. doi: 10.1109/TAC.1974.1100705.
- Bossenbroek, J.M., Johnson, L.E., Peters, B. & Lodge, D.M. (2007) Forecasting the expansion of zebra mussels in the United States. *Conservation Biology*, **21**, 800–810. doi: 10.1111/j.1523-1739.2006.00614.x.
- Bossenbroek, J.M., Kraft, C.E. & Nekola, J.C. (2001) Prediction of long-distance dispersal using gravity mod-

- els: zebra mussel invasion of inland lakes. *Ecological Applications*, **11**, 1778–1788. doi: 10.1890/1051-0761(2001)011[1778:POLDDU]2.0.CO;2.
- Burnham, K.P. & Anderson, D.R. (2004) Multimodel Inference: Understanding AIC and BIC in Model Selection. *Sociological Methods & Research*, **33**, 261–304. doi: 10.1177/0049124104268644.
- Byrd, R.H., Lu, P., Nocedal, J. & Zhu, C. (1995) A limited memory algorithm for bound constrained optimization. *SIAM Journal on Scientific Computing*, **16**, 1190–1208. doi: 10.1137/0916069.
- Chen, Y., Li, P. & Wu, C. (2020) Doubly robust inference with nonprobability survey samples. *Journal of the American Statistical Association*, **115**, 2011–2021. doi: 10.1080/01621459.2019.1677241.
- Chivers, C. & Leung, B. (2012) Predicting invasions: alternative models of human-mediated dispersal and interactions between dispersal network structure and Allee effects. *Journal of Applied Ecology*, **49**, 1113–1123. doi: 10.1111/j.1365-2664.2012.02183.x.
- Cushman, J.H. & Meentemeyer, R.K. (2008) Multi-scale patterns of human activity and the incidence of an exotic forest pathogen. *Journal of Ecology*, **96**, 766–776. doi: 10.1111/j.1365-2745.2008.01376.x.
- DFO, D.o.F.a.O.C. (2019) *Survey of recreational fishing in Canada, 2015*. Ottawa, ON. OCLC: 1199132468.
- Drake, D.A.R. & Mandrak, N.E. (2010) Least-cost transportation networks predict spatial interaction of invasion vectors. *Ecological Applications*, **20**, 2286–2299. doi: 10.1890/09-2005.1.
- Drake, D.A.R. & Mandrak, N.E. (2014) Bycatch, bait, anglers, and roads: quantifying vector activity and propagule introduction risk across lake ecosystems. *Ecological Applications*, **24**, 877–894. doi: 10.1890/13-0541.1.
- Dungan, J.L., Perry, J.N., Dale, M.R.T., Legendre, P., Citron-Pousty, S., Fortin, M.J., Jakomulska, A., Miriti, M. & Rosenberg, M.S. (2002) A balanced view of scale in spatial statistical analysis. *Ecography*, **25**, 626–640. doi: 10.1034/j.1600-0587.2002.250510.x.
- Elwell, L.C.S., Stromberg, K.E., Ryce, E.K. & Bartholomew, J.L. (2010) Whirling disease in the united states: A summary of progress in research and management. *Proceedings of the Wild Trout X Symposium, West Yellowstone, Montana*, p. 203.
- Ferrari, M.J., Bjørnstad, O.N., Partain, J.L. & Antonovics, J. (2006) A gravity model for the spread of a pollinator-borne plant pathogen. *The American Naturalist*, **168**, 294–303. doi: 10.1086/506917.
- Fischer, S.M., Beck, M., Herborg, L.M. & Lewis, M.A. (2020) A hybrid gravity and route choice model to assess vector traffic in large-scale road networks. *Royal Society Open Science*, **7**, 191858. doi: 10.1098/rsos.191858.
- Fischer, S.M. & Lewis, M.A. (2021) A robust and efficient algorithm to find profile likelihood confidence intervals. *Statistics and Computing*, **31**, 38. doi: 10.1007/s11222-021-10012-y.

- Fischer, S. M., Ramazi, P., Simmons, S., Poesch, M. S., and Lewis, M. A. (2022). Data for “Boosting propagule transport models with individual-specific data from mobile apps”. *Dryad Digital Repository*. <https://doi.org/10.5061/dryad.6m905qg3j>.
- Gates, K.K. *et al.* (2007) *Myxospore detection in soil and angler movement in southwestern Montana: implications for whirling disease transport*. Ph.D. thesis, Montana State University-Bozeman, College of Letters & Science.
- Ghosh, J. & Samanta, T. (2001) Model selection – an overview. *Current Science*, **80**, 1135.
- Hofer, B. (1903) Über die drehkrankheit der regenbogenforelle. *Allgemeine Fischerei-Zeitung*, **28**, 7–8.
- Hulme, P.E. (2009) Trade, transport and trouble: managing invasive species pathways in an era of globalization. *Journal of Applied Ecology*, **46**, 10–18. doi: 10.1111/j.1365-2664.2008.01600.x.
- Husak, G.J., Michaelsen, J. & Funk, C. (2007) Use of the gamma distribution to represent monthly rainfall in Africa for drought monitoring applications. *International Journal of Climatology*, **27**, 935–944. doi: 10.1002/joc.1441.
- Johnson, L.E., Ricciardi, A. & Carlton, J.T. (2001) Overland dispersal of aquatic invasive species: a risk assessment of transient recreational boating. *Ecological Applications*, **11**, 1789–1799. doi: 10.1890/1051-0761(2001)011[1789:ODOAIS]2.0.CO;2.
- Johnston, F.D., Simmons, S., van Poorten, B.T. & Venturelli, P.A. (2021) Comparative analyses with conventional surveys reveal the potential for an angler app to contribute to recreational fisheries monitoring. *Canadian Journal of Fisheries and Aquatic Sciences*, pp. cjfas-2021-0026. doi: 10.1139/cjfas-2021-0026.
- Jones, E., Oliphant, T. & Peterson, P. (2001) SciPy: open source scientific tools for Python. Retrieved from <https://scipy.org/>.
- Karesh, W.B., Cook, R.A., Bennett, E.L. & Newcomb, J. (2005) Wildlife trade and global disease emergence. *Emerging Infectious Diseases*, **11**, 1000–1002. doi: 10.3201/eid1107.050194.
- Kilian, J.V., Klauda, R.J., Widman, S., Kashiwagi, M., Bourquin, R., Weglein, S. & Schuster, J. (2012) An assessment of a bait industry and angler behavior as a vector of invasive species. *Biological Invasions*, **14**, 1469–1481.
- Kleiber, C. & Kotz, S. (2003) *Statistical size distributions in economics and actuarial sciences*. Wiley series in probability and statistics. Wiley, Hoboken, NJ.
- Koch, F.H., Yemshanov, D., Magarey, R.D. & Smith, W.D. (2012) Dispersal of invasive forest insects via recreational firewood: a quantitative analysis. *Journal of Economic Entomology*, **105**, 438–450. doi: 10.1603/EC11270.
- Kraft, D. (1988) A software package for sequential quadratic programming. Technical Report DFVLR-FB 88-28, DLR German Aerospace Center – Institute for Flight Mechanics, Köln, Germany.

- Lee, A. (2010) Circular data. *Wiley Interdisciplinary Reviews: Computational Statistics*, **2**, 477–486. doi: 10.1002/wics.98.
- Leung, B., Drake, J.M. & Lodge, D.M. (2004) Predicting invasions: Propagule pressure and the gravity of Allee effects. *Ecology*, **85**, 1651–1660. doi: 10.1890/02-0571.
- Leung, B. & Mandrak, N.E. (2007) The risk of establishment of aquatic invasive species: joining invasibility and propagule pressure. *Proceedings of the Royal Society B: Biological Sciences*, **274**, 2603–2609.
- Lewis, M., Petrovskii, S.V. & Potts, J.R. (2016) *The mathematics behind biological invasions*. Number 44 in Interdisciplinary applied mathematics. Springer, Cham. OCLC: 957633921.
- Li, X., Tian, H., Lai, D. & Zhang, Z. (2011) Validation of the gravity model in predicting the global spread of influenza. *International Journal of Environmental Research and Public Health*, **8**, 3134–3143. doi: 10.3390/ijerph8083134.
- Litvak, M.K. & Mandrak, N.E. (1993) Ecology of freshwater baitfish use in Canada and the United States. *Fisheries*, **18**, 6–13.
- Muirhead, J.R., Leung, B., Overdijk, C., Kelly, D.W., Nandakumar, K., Marchant, K.R. & MacIsaac, H.J. (2006) Modelling local and long-distance dispersal of invasive emerald ash borer *Agrilus planipennis* (Coleoptera) in North America. *Diversity & Distributions*, **12**, 71–79. doi: 10.1111/j.1366-9516.2006.00218.x.
- Muirhead, J.R., Lewis, M.A. & MacIsaac, H.J. (2011) Prediction and error in multi-stage models for spread of aquatic non-indigenous species: Prediction and error in multi-stage models. *Diversity and Distributions*, **17**, 323–337. doi: 10.1111/j.1472-4642.2011.00745.x.
- Muirhead, J.R. & MacIsaac, H.J. (2011) Evaluation of stochastic gravity model selection for use in estimating non-indigenous species dispersal and establishment. *Biological Invasions*, **13**, 2445–2458. doi: 10.1007/s10530-011-0070-3.
- Nagelkerke, N.J.D. (1991) A note on a general definition of the coefficient of determination. *Biometrika*, **78**, 691–692. doi: 10.1093/biomet/78.3.691.
- Nalepa, T.F. & Schloesser, D.W. (2013) *Quagga and zebra mussels: biology, impacts, and control*. CRC Press.
- Nocedal, J. & Wright, S.J. (2006) Trust-region methods. *Numerical Optimization*, pp. 66–100. Springer New York, 2nd edition.
- Papenfuss, J.T., Phelps, N., Fulton, D. & Venturelli, P.A. (2015) Smartphones reveal angler behavior: a case study of a popular mobile fishing application in Alberta, Canada. *Fisheries*, **40**, 318–327. doi: 10.1080/03632415.2015.1049693.

- Pluess, T., Cannon, R., Jarošík, V., Pergl, J., Pyšek, P. & Bacher, S. (2012) When are eradication campaigns successful? a test of common assumptions. *Biological Invasions*, **14**, 1365–1378.
- Potapov, A., Muirhead, J., Yan, N., Lele, S. & Lewis, M. (2011) Models of lake invasibility by *Bythotrephes longimanus*, a non-indigenous zooplankton. *Biological Invasions*, **13**, 2459–2476. doi: 10.1007/s10530-011-0075-y.
- Potapov, A., Muirhead, J.R., Lele, S.R. & Lewis, M.A. (2010) Stochastic gravity models for modeling lake invasions. *Ecological Modelling*, **222**, 964–972. doi: 10.1016/j.ecolmodel.2010.07.024.
- Prasad, A.M., Iverson, L.R., Peters, M.P., Bossenbroek, J.M., Matthews, S.N., Davis Sydnor, T. & Schwartz, M.W. (2010) Modeling the invasive emerald ash borer risk of spread using a spatially explicit cellular model. *Landscape Ecology*, **25**, 353–369. doi: 10.1007/s10980-009-9434-9.
- Ramazi, P., Fischer, S.M., Alexander, J., James, C., Paul, A.J., Greiner, R. & Lewis, M.A. (2021a) *M. cerebralis* establishment and spread: A graphical synthesis. *Canadian Journal of Fisheries and Aquatic Sciences*, pp. cjfas-2020-0352. doi: 10.1139/cjfas-2020-0352.
- Ramazi, P., Kunegel-Lion, M., Greiner, R. & Lewis, M.A. (2021b) Predicting insect outbreaks using machine learning: A mountain pine beetle case study. *Ecology and Evolution*, **11**, 13014–13028. doi: 10.1002/ece3.7921.
- Sorn, R. & Price, K. (1997) Differential evolution – a simple and efficient heuristic for global optimization over continuous spaces. *Journal of global optimization*, **11**, 341–359. doi: 10.1023/A:1008202821328.
- Turner, K.G., Smith, M.J. & Ridenhour, B.J. (2014) Whirling disease dynamics: an analysis of intervention strategies. *Preventive veterinary medicine*, **113**, 457–468.
- Varin, C. (2008) On composite marginal likelihoods. *AStA Advances in Statistical Analysis*, **92**, 1–28. doi: 10.1007/s10182-008-0060-7.
- Venturelli, P.A., Hyder, K. & Skov, C. (2017) Angler apps as a source of recreational fisheries data: opportunities, challenges and proposed standards. *Fish and Fisheries*, **18**, 578–595. doi: 10.1111/faf.12189.
- Villa, E.R. & Escobar, L.A. (2006) Using moment generating functions to derive mixture distributions. *The American Statistician*, **60**, 75–80. doi: 10.1198/000313006X90819.
- Von der Lippe, M. & Kowarik, I. (2007) Long-distance dispersal of plants by vehicles as a driver of plant invasions. *Conservation Biology*, **21**, 986–996. doi: 10.1111/j.1523-1739.2007.00722.x.
- Wang, F., Wang, J., Cao, J., Chen, C. & Ban, X.J. (2019) Extracting trips from multi-sourced data for mobility pattern analysis: An app-based data example. *Transportation Research Part C: Emerging Technologies*, **105**, 183–202.
- Wang, M.C. & Van Ryzin, J. (1981) A class of smooth estimators for discrete distributions. *Biometrika*, **68**, 301–309. doi: 10.1093/biomet/68.1.301.

Supporting Information for “Boosting Propagule Transport Models with Individual-Specific Data from Mobile Apps”

Samuel M. Fischer^{1,2,*}, Pouria Ramazi³, Sean Simmons⁴, Mark S. Poesch⁵, and Mark A. Lewis^{1,6}

¹*Department of Mathematical and Statistical Sciences, University of Alberta, Edmonton, AB, T6G 2G1, Canada.*

²*Department of Ecological Modelling, Helmholtz-Centre for Environmental Research - UFZ, Permoserstraße 15, 04318 Leipzig, Germany.*

³*Department of Mathematics and Statistics, Brock University, St. Catharines, ON, L2S 3A1, Canada.*

⁴*Angler’s Atlas, Goldstream Publishing, PO Box 182, Prince George, BC, V2L 4S1, Canada.*

⁵*Department of Renewable Resources, University of Alberta, Edmonton, AB, T6G 2R3, Canada.*

⁶*Department of Biological Sciences, University of Alberta, Edmonton, AB, T6G 2E9, Canada.*

**samuel.fischer@ualberta.ca*

S1 Overview of mathematical symbols used in the paper

The table below provides an overview of the mathematical symbols used in the main text.

Symbol	Explanation
i	Origin locality
j	Destination subbasin
t	Day
\mathcal{R}	Region of preference; a set of subbasins
N_t	Total number of recorded angler trips on day t
N_{ijt}	Total number of recorded angler trips from i to j on day t
$N_{ij,\text{fit}}$	Total number of recorded angler trips from i to j in the training dataset
$N_{ij,\text{val}}$	Total number of recorded angler trips from i to j in the validation dataset
$\bar{N}_{ij,\text{fit}}$	Empirical estimate for the <i>annual</i> number of recorded angler trips from i to j based on the training data
$\bar{N}_{ij,\text{val}}$	Empirical estimate for the <i>annual</i> number of recorded angler trips from i to j based on the validation data
n_i	Number of anglers residing at locality i
\tilde{n}_i	Number of app-using anglers residing at locality i
T	Number of days in the study period
\mathfrak{R}	Set of all potential regions of preference
\mathcal{X}	Group of origin or destination covariates that jointly lead to high traffic; a set of covariates
\mathbf{x}	Covariate; vector of covariate values

Symbol	Explanation
μ_i	Mean <i>daily</i> number of trips <i>per angler</i> from origin i
$\bar{\mu}$	Mean total <i>daily</i> number of recorded trips
$\mu_{j_1 j_2}$	Mean total <i>yearly</i> number of trips anglers make to destination j_1 directly after visiting destination j_2
$\mu_{i j_1 j_2}$	Mean total <i>yearly</i> number of directly consecutive trips from origin i to destinations j_1 and j_2
p_{ij}	Probability that an angler from origin i visits destination j
$p_{i\mathcal{R}}$	Probability that an angler from origin i has \mathcal{R} as region of preference
$p_{ij \mathcal{R}}$	Probability that an angler from origin i with region of preference \mathcal{R} visits destination j
ε_t	Suitability of day t for going fishing
τ_t	Expected suitability of day t
α	Dispersion parameter
ξ_{same}	Probability to revisit the previous destination
ξ_{region}	Probability to constrain the destination choice to the region of preference
ν_{app}	Probability to use the app
ν_{record}	Probability to record a trip
a_j	Attractiveness of destination j
D	Distance decay function for the destination choice probabilities
f_{vM}	Probability density function of the von Mises distribution
c	Scaling constant for the mean number of trips per day
C	Scaling constant for the mean number of <i>recorded</i> trips per day
c_{norm}	Normalization constant for the mean day suitability
ρ	Radius of the inscribed circle of regions of preference
δ_0	Distance of half choice-probability decay
c_{week}	Week addition constant
θ_{week}	Week location constant
κ_{week}	Week shape constant
c_{year}	Year addition constant
θ_{year}	Year location constant
κ_{year}	Year shape constant
$\beta_{\mathbf{x}}$	Scaling parameter for covariate \mathbf{x}
$\gamma_{\mathbf{x}}$	Power parameter for covariate \mathbf{x}
ω_{fit}	Fraction of the data used for fitting the model
ω_{val}	Fraction of the data used for model validation
$\delta_{j_1 j_2}$	Kronecker delta; 1 if $j_1 = j_2$ and 0 otherwise

S2 Computing the expected number of trips between angler destinations

Below, we show how the mean number of consecutive trips to two destinations can be computed efficiently. As described in the main text, the mean number of consecutive trips to two destinations j_1 and j_2 by anglers from origin i is given by

$$\begin{aligned} \mu_{ij_1j_2} = n_i \mu_i T & \left(\xi_{\text{same}} \delta_{j_1j_2} p_{ij_1} + (1 - \xi_{\text{same}}) \left(\xi_{\text{all}}^2 p_{ij_1} p_{ij_2} + \xi_{\text{all}} \xi_{\text{region}} p_{ij_1} \sum_{\mathcal{R}: j_2 \in \mathcal{R}} p_{i\mathcal{R}} p_{ij_2|\mathcal{R}} \right. \right. \\ & \left. \left. + \xi_{\text{region}} \xi_{\text{all}} p_{ij_2} \sum_{\mathcal{R}: j_1 \in \mathcal{R}} p_{i\mathcal{R}} p_{ij_1|\mathcal{R}} + \xi_{\text{region}}^2 \sum_{\mathcal{R}: j_1, j_2 \in \mathcal{R}} p_{i\mathcal{R}} p_{ij_1|\mathcal{R}} p_{ij_2|\mathcal{R}} \right) \right). \quad (\text{S1}) \end{aligned}$$

After expanding and simplifying equation (S1), we obtain

$$\begin{aligned} \mu_{ij_1j_2} = n_i \mu_i T & \left(\xi_{\text{same}} \delta_{j_1j_2} p_{ij_1} + (1 - \xi_{\text{same}}) \left(\xi_{\text{all}}^2 p_{ij_1} p_{ij_2} + \xi_{\text{all}} \xi_{\text{region}} \sum_{\mathcal{R}: j_2 \in \mathcal{R}} \frac{p_{ij_1} p_{ij_2}}{\sum_{\tilde{\mathcal{R}}} \sum_{j \in \tilde{\mathcal{R}}} p_{ij}} \right. \right. \\ & \left. \left. + \xi_{\text{all}} \xi_{\text{region}} p_{ij_2} \sum_{\mathcal{R}: j_1 \in \mathcal{R}} \frac{p_{ij_1} p_{ij_2}}{\sum_{\tilde{\mathcal{R}}} \sum_{j \in \tilde{\mathcal{R}}} p_{ij}} + \xi_{\text{region}}^2 \sum_{\mathcal{R}: j_1, j_2 \in \mathcal{R}} \frac{p_{ij_1} p_{ij_2}}{\sum_{j \in \mathcal{R}} p_{ij} \cdot \sum_{\tilde{\mathcal{R}}} \sum_{j \in \tilde{\mathcal{R}}} p_{ij}} \right) \right) \\ = n_i \mu_i T p_{ij_1} & \left(\xi_{\text{same}} \delta_{j_1j_2} + (1 - \xi_{\text{same}}) p_{ij_2} \left(\xi_{\text{all}}^2 + \frac{1}{\sum_{\tilde{\mathcal{R}}} \sum_{j \in \tilde{\mathcal{R}}} p_{ij}} \left(\right. \right. \right. \\ & \left. \left. \xi_{\text{all}} \xi_{\text{region}} (|\{\mathcal{R} : j_1 \in \mathcal{R}\}| + |\{\mathcal{R} : j_2 \in \mathcal{R}\}|) + \xi_{\text{region}}^2 \sum_{\mathcal{R}: j_1, j_2 \in \mathcal{R}} \frac{1}{\sum_{j \in \mathcal{R}} p_{ij}} \right) \right) \right), \quad (\text{S2}) \end{aligned}$$

where $|\cdot|$ denotes the counting norm. The right hand side of (S2) can be evaluated efficiently for all origins i and destinations j_1 and j_2 if the individual terms are stored for reuse.

S3 Likelihood derivation

Here, we show how the likelihood functions used in the model fitting stages are derived and how they can be computed efficiently.

S3.1 Day suitability

In this section, we derive the likelihood function for the distribution of trips recorded each day N_t . Recall that the rate of trips for anglers from origin i on day t is assumed to be $\mu_i \varepsilon_t$. As a result, the number of trips that such anglers make on day t is Poisson distributed with mean $\mu_i \varepsilon_t$. Since ε_t follows a gamma

distribution with shape parameter $\frac{\tau_t}{\alpha}$ and scale parameter α , the distribution of the total number \bar{N}_t of trips on day t is

$$\begin{aligned}\bar{N}_t &\sim \sum_i \sum_{k=1}^{n_i} \text{Poisson}(\mu_i \varepsilon_t) \\ &= \sum_i \text{Poisson}(n_i \mu_i \varepsilon_t) \\ &= \text{Poisson}\left(\varepsilon_t \sum_i n_i \mu_i\right),\end{aligned}\tag{S3}$$

which in turn is a negative binomial distribution with dispersion parameter $\frac{\alpha}{\tau_t}$ and mean $\tau_t \sum_i n_i \mu_i$ (Villa & Escobar, 2006).

When computing the likelihood of our observed data, we need to take into account that many anglers are not using the app. Consequently, we need to use the number \tilde{n}_i of app users in locality i instead of the angler number n_i . As \tilde{n}_i is a random variable itself, we were not able to derive a closed-form solution of the exact likelihood function. However, since we consider the *total* number of trips each day, the identities of the individual anglers who made the trips is of minor importance, and we may consider the individual trips on a day as independent from one another. This approximation is appropriate, because we consider a large number of anglers and a relatively small number of trips. The number of trips recorded via the app is then

$$N_t \sim \text{Binomial}(\bar{N}_t, \nu_{\text{app}} \nu_{\text{record}}).\tag{S4}$$

This can be expressed as a negative binomial distribution with dispersion parameter $\frac{\alpha}{\tau_t}$ and mean $\tau_t \bar{\mu}$, where $\bar{\mu} = \nu_{\text{app}} \nu_{\text{record}} \sum_i n_i \mu_i$ (Villa & Escobar, 2006).

Let k_t denote the number of trips recorded on day t . Following the derivation above, the likelihood function then reads

$$L_{\text{time}} = \prod_t \binom{k_t + \frac{\tau_t}{\alpha} - 1}{\frac{\tau_t}{\alpha} - 1} \left(\frac{1}{1 + \alpha \bar{\mu}}\right)^{\frac{\tau_t}{\alpha}} \left(\frac{\alpha \bar{\mu}}{1 + \alpha \bar{\mu}}\right)^{k_t}.\tag{S5}$$

The log-likelihood function (disregarding an irrelevant constant shifting term) is

$$\ell_{\text{time}} = \sum_t \ln \Gamma\left(k_t + \frac{\tau_t}{\alpha}\right) - \sum_t \ln \Gamma\left(\frac{\tau_t}{\alpha}\right) + K (\ln \alpha + \ln \bar{\mu}) - \left(\frac{T}{\alpha} + K\right) \ln(1 + \alpha \bar{\mu}),\tag{S6}$$

where $T = \sum_t \tau_t$ is the number of days in the study period, and $K = \sum_t k_t$ is the total number of observed trips. Note that days t with $k_t = 0$ can be omitted in the sums in (S6) without changing ℓ_{time} .

S3.2 Angler activeness and destination choice probabilities

The likelihood function for the stochastic gravity model yielding the angler activeness and the destination choice probabilities can be derived analogously to the likelihood function for the day suitability. Again, we consider individual trips on a day as independent from one another to improve the computational performance. Then, the number of trips between each origin-destination pair is negative binomially distributed. Since it is difficult to account for the stochastic dependency of angler counts on the same day, we also assume that the traveller counts between each origin and destination are mutually independent.

To derive the likelihood function, let $\check{\mu}_i = \mu_i/c$, where μ_i and c are defined as in equation (9) (main text). The mean number of recorded trips from origin i to destination j on day t is

$$\begin{aligned}\mu_{ijt} &= \tau_t n_i \mu_i p_{ij} \nu_{\text{app}} \nu_{\text{record}} \\ &= C \tau_t n_i \check{\mu}_i p_{ij}.\end{aligned}\tag{S7}$$

Here, τ_t and n_i are already estimated or known, $\check{\mu}_i$ and p_{ij} are functions of parameters and covariates (see equations (7)-(8) in the main text), and $C = \nu_{\text{app}} \nu_{\text{record}} c$ is the product of not individually identifiable parameters. The dispersion parameter of the distribution is $\frac{\alpha}{\tau_t}$. With k_{ijt} being the number of recorded trips from origin i to destination j on day t , we obtain the likelihood function

$$L_{\text{gravity}} = \prod_{i,j,t} \binom{k_{ijt} + \frac{\tau_t}{\alpha} - 1}{\frac{\tau_t}{\alpha} - 1} \left(\frac{1}{1 + \alpha C n_i \check{\mu}_i p_{ij}} \right)^{\frac{\tau_t}{\alpha}} \left(\frac{\alpha C n_i \check{\mu}_i p_{ij}}{1 + \alpha C n_i \check{\mu}_i p_{ij}} \right)^{k_{ijt}}\tag{S8}$$

and the log-likelihood function (up to a constant shifting term)

$$\begin{aligned}\ell_{\text{gravity}} &= \sum_{i,j,t} \ln \Gamma \left(k_{ijt} + \frac{\tau_t}{\alpha} \right) - \sum_{i,j,t} \ln \Gamma \left(\frac{\tau_t}{\alpha} \right) + \sum_{i,j,t} k_{ijt} \ln (\alpha C n_i \check{\mu}_i p_{ij}) \\ &\quad - \sum_{i,j,t} \left(\frac{\tau_t}{\alpha} + k_{ijt} \right) \ln (1 + \alpha C n_i \check{\mu}_i p_{ij})\end{aligned}\tag{S9}$$

$$\begin{aligned}&= \sum_{i,j,t: k_{ijt} \neq 0} \ln \Gamma \left(k_{ijt} + \frac{\tau_t}{\alpha} \right) - \sum_t k_t \ln \Gamma \left(\frac{\tau_t}{\alpha} \right) - \frac{T}{\alpha} \sum_{i,j} \ln (1 + \alpha C n_i \check{\mu}_i p_{ij}) \\ &\quad + \sum_{i,j: k_{ij} \neq 0} k_{ij} \ln (\alpha C n_i \check{\mu}_i p_{ij}) - \sum_{i,j,t: k_{ijt} \neq 0} k_{ijt} \ln (1 + \alpha C n_i \check{\mu}_i p_{ij}).\end{aligned}\tag{S10}$$

Here, $k_{ij} = \sum_t k_{ijt}$ is the total number of trips observed from origin i to destination j . The time required to evaluate ℓ_{gravity} is dominated by either the number of origin-destination pairs or the number of recorded

trips.

S3.3 Choice parameters

To derive the likelihood for the remaining choice parameters, we express the negative binomial probability mass function in a simpler way in terms of the parameters $q = \frac{1}{1+\bar{\alpha}\mu}$, describing the distribution's mean-to-variance ratio, and the parameter $r = \frac{1}{\alpha}$, which is proportional to the distribution's expected value. Here, μ refers to the distribution's expected value and $\bar{\alpha}$ to respective dispersion parameter. With the changed parameterization, the probability mass function of the negative binomial distribution reads

$$f(k; r, q) = \binom{k+r-1}{r-1} q^r (1-q)^k. \quad (\text{S11})$$

In contrast to the previous section, we need to consider the decisions of each angler individually, to fit the remaining parameters. Consider an angler from origin i who uses the app and recorded trips on days t_1, \dots, t_m to the destinations j_1, \dots, j_m . To compute the likelihood for this sequence of trips, we first determine the probability that the angler records trips on the days t_1, \dots, t_m . Then we compute the probability that they choose the recorded locations j_1, \dots, j_m given that they recorded trips on days t_1, \dots, t_m .

Let k_t be the number of trips that the angler has made on day t , and define $\tilde{q}_i = 1/(1 + \alpha\nu_{\text{record}}\mu_i)$ and $r_t = \frac{t_t}{\alpha}$. The probability that we observe the given sequence of trips by the angler (ignoring the destinations) is

$$\prod_t \binom{k_t + r_t - 1}{r_t - 1} \tilde{q}_i^{r_t} (1 - \tilde{q}_i)^{k_t}, \quad (\text{S12})$$

which can be written as

$$\tilde{q}_i^{T/\alpha} \prod_{t: k_t \neq 0} \binom{k_t + r_t - 1}{r_t - 1} (1 - \tilde{q}_i)^{k_t}. \quad (\text{S13})$$

Now we proceed with the second step and derive the probability for a particular sequence of destination choices given the dates of the corresponding trips. We have to take into account that the angler may have made additional intermediate trips between any consecutive pair of recorded trips. We start by deriving the probability $p_{i,j_l,j_{l+1}|\mathcal{R},k}$ that an angler from locality i with preferred fishing region \mathcal{R} records a trip to site j_{l+1} , given that (1) the trip they recorded had the destination j_l and (2) that they took $k-1$ trips between the recorded trips. Recall that on each trip, the angler can either (A) refuse to choose a new destination and choose the last destination again, (B) restrict the destination choice to their region of

preference \mathcal{R} , or (C) make an unrestricted choice from all available destinations. Now note the following:

1. The probability that the angler refuses to choose a new destination for all k trips is $\delta_{j_l j_{l+1}} \xi_{\text{same}}^k$. Recall that $\delta_{j_l j_{l+1}}$ is 1 if $j_l = j_{l+1}$ and 0 else. The delta multiplier is necessary, because the probability that the angler chooses the same destination for all k intermediate trips is 0 if the first and the final destination are not equal.
2. The probability that the angler chooses a new destination for at least one of the k trips is $1 - (1 - \delta_{1l}) \xi_{\text{same}}^k$. Here, the term $1 - \delta_{1l}$ models that on their very first trip, the angler cannot choose the same destination as on a previous trip.
3. Suppose the angler chooses a new destination for at least one of the k trips and consider among these trips the last one for which the angler chooses a new destination. The probability that they make an unconstrained destination choice and choose j_{l+1} as destination on this trip is $\xi_{\text{all}} p_{ij_{l+1}}$.
4. Under the same conditions as described in point 3, the probability that – on the last trip where they choose a new destination – the angler restricts their destination choice to their preferred region and chooses j_l is $\mathbb{I}_{\mathcal{R}}(j_{l+1}) \xi_{\text{region}} p_{ij_{l+1}|\mathcal{R}}$. Here, $\mathbb{I}_{\mathcal{S}}(s)$ is the indicator function, which is 1 if $s \in \mathcal{S}$ and 0 else.

Putting the above observations together, we obtain

$$p_{ij_l j_{l+1}|\mathcal{R},k} = \left(1 - (1 - \delta_{1l}) \xi_{\text{same}}^k\right) (\xi_{\text{all}} p_{ij_{l+1}} + \mathbb{I}_{\mathcal{R}}(j_{l+1}) \xi_{\text{region}} p_{ij_{l+1}|\mathcal{R}}) + \delta_{j_l j_{l+1}} \xi_{\text{same}}^k. \quad (\text{S14})$$

Since $p_{ij_l j_{l+1}|\mathcal{R},k}$ depends on the (unknown) number of intermediate trips between two recorded trips, we need to derive the distribution of this number. Let $\mathcal{T} = \{t \in \mathbb{N} : t_l < t < t_{l+1}\}$ be the set of days between the recorded trips l and $l+1$. If $l = 0$, set t_0 as the last day before the study period started. The number of trips that the angler makes during the days in \mathcal{T} is negative binomially distributed with the parameters

$$\bar{r}_{\mathcal{T}} = \frac{1}{\alpha} \sum_{t \in \mathcal{T}} \tau_t \quad (\text{S15})$$

$$q_i = \frac{1}{1 + \alpha \mu_i}. \quad (\text{S16})$$

The distribution of unrecorded trips within the days in \mathcal{T} is described by

$$\begin{aligned} \mathbb{P}(k \text{ trips during } \mathcal{T} \mid \text{no trip recorded}) &= \frac{\mathbb{P}(k \text{ trips during } \mathcal{T}) (1 - \nu_{\text{record}})^k}{\mathbb{P}(\text{no trips recorded during } \mathcal{T})} \\ &= \binom{k + \bar{r}_{\mathcal{T}} - 1}{\bar{r}_{\mathcal{T}} - 1} (1 - (1 - \nu_{\text{record}})(1 - q_i))^{\bar{r}_{\mathcal{T}}} ((1 - \nu_{\text{record}})(1 - q_i))^k. \end{aligned} \quad (\text{S17})$$

The factor $(1 - (1 - \nu_{\text{record}})(1 - q_i))^{\bar{r}_{\mathcal{T}}}$ normalizes the distribution so that the probabilities for all $k \in \mathbb{N}$ sum to 1.

The distribution given by (S17) describes the number of unrecorded trips during *complete* days between two trip records. However, multiple trips can be made on the same day. In particular, the considered angler could have made unrecorded intermediate trips on the days t_l and t_{l+1} . Though multiple trips on the same day may occur rarely only, overdispersed distributions have the property that the probability for a second trip (given that a first trip has been made) is higher than the unconditional probability for a first trip. Therefore, ignoring the possibility of unrecorded trips on the days t_l and t_{l+1} would skew the likelihood significantly.

Below, we will first derive the distribution of unrecorded trips on a day where a trip has already been recorded. Afterwards, we determine the joint distribution of unrecorded trips, before we finally incorporate the probabilities to choose specific locations and determine the likelihood function. Consider a day t on which the angler makes $M_t \geq N_t$ trips, where they record $N_t \geq 1$ of these trips. Partition the day into time intervals separated by the recorded trips and consider any of the arising sections. Let k be the number of unrecorded trips made during this day section. The number of possibilities to distribute the remaining unrecorded trips over the other, remaining sections is

$$\binom{M_t - k - 1}{N_t - 1}, \quad (\text{S18})$$

as can be computed with the stars and bars method. As a result, the probability that the angler makes k unrecorded trips in this time interval is

$$\mathbb{P}(k \text{ unrecorded trips in section} \mid M_t \text{ total trips; } N_t \text{ recorded trips}) = \frac{\binom{M_t - k - 1}{N_t - 1}}{\binom{M_t}{N_t}}. \quad (\text{S19})$$

The normalization factor was obtained by summing over all $k \in \mathbb{N}$.

The number of trips recorded on the considered day follows a binomial distribution with parameters M and ν_{record} ; the total number M of trips follows a negative binomial distribution with parameters

$r_t = \frac{\tau_t}{\alpha}$ and $q_i = \frac{1}{1+\alpha\mu_i}$. Hence, the joint probability that an angler makes k unrecorded trips between two recorded trips if they recorded N_t trips in total is

$$\begin{aligned}
& \mathbb{P}(k \text{ unrecorded trips on day } t \mid N_t \text{ trips recorded on day } t) \\
&= \bar{C} \sum_{M_t=N_t+k}^{\infty} \underbrace{\binom{M_t+r_t-1}{r_t-1} q_i^{r_t} (1-q_i)^{M_t}}_{\mathbb{P}(\text{make } M_t \text{ trips})} \underbrace{\binom{M_t}{N_t} \nu_{\text{record}}^{N_t} (1-\nu_{\text{record}})^{m-N_t}}_{\mathbb{P}(\text{record } N_t \text{ out of } M_t \text{ trips})} \underbrace{\binom{M_t-k-1}{N_t-1}}_{\mathbb{P}(\text{make } k \text{ unreported trips})} / \binom{M_t}{N_t} \\
&= \tilde{C} \sum_{M_t=N_t+k}^{\infty} \binom{M_t+r_t-1}{r_t-1} \binom{M_t-k-1}{N_t-1} ((1-q_i)(1-\nu_{\text{record}}))^{M_t}. \\
&= \tilde{C} \eta_i^{k+N_t} \binom{k+N_t+r_t-1}{r_t-1} {}_2F_1(N_t, k+N_t+r_t; k+N_t+1; \eta_i) \tag{S20}
\end{aligned}$$

where $\eta_i = (1-q_i)(1-\nu_{\text{record}})$, \bar{C} and \tilde{C} are normalization constants, and ${}_2F_1(\cdot, \cdot; \cdot; \cdot)$ is Gauss's hypergeometric function. To derive the normalization constant \tilde{C} , we sum over all $k \in \mathbb{N}$:

$$\begin{aligned}
\tilde{C} &= \sum_{k=0}^{\infty} \sum_{M_t=N_t+k}^{\infty} \binom{M_t+r_t-1}{r_t-1} \binom{M_t-k-1}{N_t-1} \eta_i^{M_t} \\
&= \sum_{M_t=N_t}^{\infty} \binom{M_t+r_t-1}{r_t-1} \eta_i^{M_t} \sum_{k=0}^{M_t-N_t} \binom{M_t-k-1}{N_t-1} \\
&= \sum_{M_t=N_t}^{\infty} \binom{M_t+r_t-1}{r_t-1} \eta_i^{M_t} \binom{M_t}{N_t} \\
&= \binom{N_t+r_t-1}{r_t-1} \frac{\eta_i^{N_t}}{(1-\eta_i)^{N_t+r_t}}. \tag{S21}
\end{aligned}$$

Thus,

$$\begin{aligned}
& \mathbb{P}(k \text{ unrecorded trips on day } t \mid N_t \text{ trips recorded on day } t) \\
&= \frac{\binom{N_t+k+r_t-1}{r_t-1}}{\binom{N_t+r_t-1}{r_t-1}} \eta_i^k (1-\eta_i)^{N_t+r_t} {}_2F_1(N_t, k+N_t+r_t; k+N_t+1; \eta_i). \tag{S22}
\end{aligned}$$

With this result, we can proceed deriving the joint distribution of unrecorded intermediate trips between two recorded trips. Let $f_s(k; t, N_t)$ be the probability mass function for the number of unrecorded trips in one ‘‘section’’ of day t given that N_t trips were recorded on the day. Let furthermore $f_d(k; i, \mathcal{T})$ be the probability mass function of the random variable modelling the number of unrecorded trips during the set \mathcal{T} of complete days. Let $\mathcal{T}_{t_l t_{l+1}}$ be the set of days between t_l and t_{l+1} . Then the probability mass

function of unrecorded intermediate trips is

$$f_{\text{intm}}(k; i, t_l, t_{l+1}, N_{t_l}, N_{t_{l+1}}) = \begin{cases} f_s(k; i, t_l, N_{t_l}) & \text{if } t_l = t_{l+1}, \\ \left(f_s(\tilde{k}; i, t_l, N_{t_{l+1}}) * f_s(\tilde{k}; i, t_{l+1}, N_{t_{l+1}}) \right)(k) & \text{if } t_{l+1} - t_l = 1, \\ \left(f_s(\tilde{k}; i, t_l, N_{t_{l+1}}) * f_s(\tilde{k}; i, t_{l+1}, N_{t_{l+1}}) * f_d(\tilde{k}; i, \mathcal{T}_{t_l t_{l+1}}) \right)(k) & \text{else,} \end{cases} \quad (\text{S23})$$

where “*” denotes the discrete convolution in \tilde{k} .

To determine the likelihood for an observed sequence of trips, we need to sum over all possible numbers of unrecorded trips. That is, we desire to determine

$$p_{ij_l j_{l+1} | \mathcal{R}, t_l, t_{l+1}, N_{t_l}, N_{t_{l+1}}} = \sum_{k=0}^{\infty} f_{\text{intm}}(k; i, t_l, t_{l+1}, N_{t_l}, N_{t_{l+1}}) p_{ij_l j_{l+1} | \mathcal{R}, k+1}. \quad (\text{S24})$$

Note that the argument k of f_{intm} refers to the number of intermediate unrecorded trips, whereas the corresponding subscript of $p_{ij_l j_{l+1} | \mathcal{R}, k+1}$ refers to the total number of trips (i.e. all unrecorded trips and one recorded trip).

To compute (S24) efficiently, we write

$$p_{ij_l j_{l+1} | \mathcal{R}, k+1} = \omega_{ij_{l+1} \mathcal{R}} + \psi_{ij_l j_{l+1} \mathcal{R}} \xi_{\text{same}}^{k+1} \quad (\text{S25})$$

with

$$\omega_{ij_{l+1} \mathcal{R}} = \xi_{\text{all}} p_{ij_{l+1}} + \mathbf{I}_{\mathcal{R}}(j_{l+1}) \xi_{\text{region}} p_{ij_{l+1} | \mathcal{R}} \quad (\text{S26})$$

$$\psi_{ij_l j_{l+1} \mathcal{R}} = (1 - \delta_{ll}) \left(\xi_{\text{all}} p_{ij_{l+1}} + \mathbf{I}_{\mathcal{R}}(j_{l+1}) \xi_{\text{region}} p_{ij_{l+1} | \mathcal{R}} \right) + \delta_{j_l j_{l+1}}. \quad (\text{S27})$$

Then,

$$\begin{aligned} p_{ij_l j_{l+1} | \mathcal{R}, t_l, t_{l+1}, N_{t_l}, N_{t_{l+1}}} &= \sum_{k=0}^{\infty} f_{\text{intm}}(k; i, t_l, t_{l+1}, N_{t_l}, N_{t_{l+1}}) \left(\omega_{ij_{l+1} \mathcal{R}} + \psi_{ij_l j_{l+1} \mathcal{R}} \xi_{\text{same}}^{k+1} \right) \\ &= \omega_{ij_{l+1} \mathcal{R}} + \psi_{ij_l j_{l+1} \mathcal{R}} \Upsilon_{t_l t_{l+1} N_{t_l} N_{t_{l+1}}} \Lambda_{t_l t_{l+1} N_{t_l} N_{t_{l+1}}} \end{aligned}$$

with

$$\Upsilon_{it_l t_{l+1} N_{t_l} N_{t_{l+1}}} = \begin{cases} \tilde{g}_s(i, t_l, N_{t_l}) & \text{if } t_l = t_{l+1}, \\ \tilde{g}_s(i, t_l, N_{t_l}) \tilde{g}_s(i, t_{l+1}, N_{t_{l+1}}) & \text{if } t_{l+1} - t_l = 1 \\ (1 - \eta_i)^{\bar{r}\tau_{t_l t_{l+1}}} \tilde{g}_s(i, t_l, N_{t_l}) \tilde{g}_s(i, t_{l+1}, N_{t_{l+1}}) & \text{else,} \end{cases} \quad (\text{S28})$$

$$\Lambda_{it_l t_{l+1} N_{t_l} N_{t_{l+1}}} = \begin{cases} \sum_{k=0}^{\infty} \tilde{f}_s(\tilde{k}; i, t_l, N_{t_l}) \xi_0^{k+1} & \text{if } t_l = t_{l+1}, \\ \sum_{k=0}^{\infty} \left(\tilde{f}_s(\tilde{k}; i, t_l, N_{t_l}) * \tilde{f}_s(\tilde{k}; i, t_{l+1}, N_{t_{l+1}}) \right) (k) \xi_0^{k+1} & \text{if } t_{l+1} - t_l = 1 \\ \sum_{k=0}^{\infty} \left(\tilde{f}_s(\tilde{k}; i, t_l, N_{t_l}) * \tilde{f}_s(\tilde{k}; i, t_{l+1}, N_{t_{l+1}}) * \binom{\tilde{k} + \bar{r}\tau_{t_l t_{l+1}} - 1}{\bar{r}\tau_{t_l t_{l+1}} - 1} \right) (k) \xi_0^{k+1} & \text{else,} \end{cases} \quad (\text{S29})$$

and

$$\tilde{g}_s(i, t, N_t) = (1 - \eta_i)^{N_t + r_t} \left(\binom{N_t + r_t - 1}{r_t - 1} \right)^{-1} \quad (\text{S30})$$

$$\tilde{f}_s(i, k; t, N_t) = \binom{N_t + k + r_t - 1}{r_t - 1} {}_2F_1(N_t, k + N_t + r_t; k + N_t + 1; \eta_i) \eta_i^k. \quad (\text{S31})$$

For each combination of origin i , day t , and recorded number of trips N_t we need to evaluate $\tilde{g}_s(i, t, N_t)$ and $\tilde{f}_s(k; i, t, N_t)$ only once. The same applies to day- and record-number pairs and $\Upsilon_{t_l t_{l+1} N_{t_l} N_{t_{l+1}}}$ and $\Lambda_{t_l t_{l+1} N_{t_l} N_{t_{l+1}}}$. This can help to speed up computations, if multiple anglers have recorded the same numbers of trips (typically one) on the same days. As we are not aware of a closed-form expression for the series $\Lambda_{it_1 t_2 N_1 N_2}$, we cannot compute it exactly. However, if we only consider a moderate number of terms, the truncation error is very small. We considered the first 200 terms of the sum.

With the above result, we can proceed deriving the joint likelihood for a sequence of observations. First, recall the likelihood for the temporal sequence of trips derived in equation (S12). Second, note that since we do not know the anglers' preferred fishing region, we need to sum over all region candidates \mathcal{R} to determine the correct joint probability for multiple observations. Furthermore, we need to consider that not all anglers are using the app. The probability that a sequence j_1, \dots, j_m of trips is recorded by the

app for an angler from locality i is then

$$p_{ij_1 \dots j_m} = \nu_{\text{app}} \tilde{q}_i^{T/\alpha} \prod_{t: k_t \neq 0} \binom{k_t + r_t - 1}{r_t - 1} (1 - \tilde{q}_i)^{k_t} \sum_{\mathcal{R}} p_{i\mathcal{R}} \prod_{l=1}^m \left(\omega_{ij_l \mathcal{R}} + \psi_{ij_l j_{l+1} \mathcal{R}} \Upsilon_{t_l t_{l+1} N_{t_l} N_{t_{l+1}}} \Lambda_{t_l t_{l+1} N_{t_l} N_{t_{l+1}}} \right) \quad (\text{S32})$$

with $\tilde{q}_i = 1 / (1 + \bar{\alpha} \nu_{\text{record}} \mu_i)$.

It is inefficient to sum over all potential regions of preference as suggested in equation (S32), but this is not necessary to compute the likelihood. Note that $\omega_{ij_l \mathcal{R}}$ and $\psi_{ij_l j_{l+1} \mathcal{R}}$ are independent of the region \mathcal{R} if the destination j_{l+1} is not in \mathcal{R} . Let $\mathfrak{R}_j = \{\mathcal{R} | j \in \mathcal{R}\}$ be the set of all regions that contain the destination j . Then,

$$\begin{aligned} & \sum_{\mathcal{R}} p_{i\mathcal{R}} \prod_{l=1}^m \left(\omega_{ij_l \mathcal{R}} + \psi_{ij_l j_{l+1} \mathcal{R}} \Upsilon_{t_l t_{l+1} N_{t_l} N_{t_{l+1}}} \Lambda_{t_l t_{l+1} N_{t_l} N_{t_{l+1}}} \right) \\ &= \sum_{\mathcal{R} \in \bigcup_l \mathfrak{R}_l} p_{i\mathcal{R}} \prod_{l=1}^m \left(\omega_{ij_l \mathcal{R}} + \psi_{ij_l j_{l+1} \mathcal{R}} \Upsilon_{t_l t_{l+1} N_{t_l} N_{t_{l+1}}} \Lambda_{t_l t_{l+1} N_{t_l} N_{t_{l+1}}} \right) \\ & \quad + \sum_{\mathcal{R} \notin \bigcup_l \mathfrak{R}_l} p_{i\mathcal{R}} \prod_{l=1}^m \left(\omega_{ij_l \emptyset} + \psi_{ij_l j_{l+1} \emptyset} \Upsilon_{t_l t_{l+1} N_{t_l} N_{t_{l+1}}} \Lambda_{t_l t_{l+1} N_{t_l} N_{t_{l+1}}} \right) \\ &= \sum_{\mathcal{R} \in \bigcup_l \mathfrak{R}_l} p_{i\mathcal{R}} \prod_{l=1}^m \left(\omega_{ij_l \mathcal{R}} + \psi_{ij_l j_{l+1} \mathcal{R}} \Upsilon_{t_l t_{l+1} N_{t_l} N_{t_{l+1}}} \Lambda_{t_l t_{l+1} N_{t_l} N_{t_{l+1}}} \right) \\ & \quad + \left(1 - \sum_{\mathcal{R} \in \bigcup_l \mathfrak{R}_l} p_{i\mathcal{R}} \right) \prod_{l=1}^m \left(\omega_{ij_l \emptyset} + \psi_{ij_l j_{l+1} \emptyset} \Upsilon_{t_l t_{l+1} N_{t_l} N_{t_{l+1}}} \Lambda_{t_l t_{l+1} N_{t_l} N_{t_{l+1}}} \right) \end{aligned} \quad (\text{S33})$$

with

$$\omega_{ij_l \emptyset} = p_{ij_{l+1}} \xi_{\text{all}} \quad (\text{S34})$$

$$\psi_{ij_l j_{l+1} \emptyset} = \delta_{j_l j_{l+1}} - (1 - \delta_{1l}) p_{ij_{l+1}} \xi_{\text{all}}. \quad (\text{S35})$$

Since $\bigcup_l \mathfrak{R}_l$ is typically small, the sum (S33) can be computed efficiently.

If no trip was observed for an angler, this may have three causes: (1) the angler may not use the app, (2) the angler may have decided not to record any of their trips, and (3) the angler may not have made

any trips. Hence, the probability to record no trip by an angler from origin i is

$$p_{i\emptyset} = (1 - \nu_{\text{app}}) + \nu_{\text{app}} \tilde{q}_i^{T/\alpha}. \quad (\text{S36})$$

The overall joint likelihood function of our model is the product of the probabilities $p_{ij_1 \dots j_m}$ or $p_{i\emptyset}$ for all anglers.

The likelihood function derived above does not include the parameter ν_{app} , since anglers who do not use the app would not be in our dataset. In turn, the likelihood function includes the parameter μ_i , which could only be estimated up to a proportionality constant in the previous step. Nonetheless, both ν_{app} and μ_i can be estimated via our model. Recall from Appendix S3.2 that we are able to estimate the constant $C = \nu_{\text{app}} \nu_{\text{record}} c$, where c is the proportionality constant of μ_i . The constant ν_{record} occurs in the likelihood function described and may thus be estimated. Furthermore, the likelihood function includes μ_i , which can be written as $\mu_i = c \tilde{\mu}_i$, where $\tilde{\mu}_i$ has is estimated via the gravity model (see Appendix S3.2). Hence, c appears in the likelihood function as a free parameter and may thus be estimated. With the estimates of ν_{record} , c , and C , however, the fraction of app users ν_{app} can be computed directly. That is, all parameters of the model may be estimable.

S4 Details about the procedures applied to optimize likelihood and AIC

In this appendix, we provide details about the procedures we applied to maximize the likelihood functions and to select the model with the minimal AIC value.

S4.1 Likelihood maximization

To maximize the likelihood, we used a number of different optimizations algorithms with different strengths that we applied consecutively. For all submodels, we started with a meta-heuristic global search algorithm in a generous subspace of the parameter space. Specifically, we used the “differential evolution” algorithm by [Storn & Price \(1997\)](#). As this algorithm converges only slowly, we terminated it after a moderate number of iterations. Then we proceeded with the L-BFGS-G algorithm ([Byrd *et al.*, 1995](#)), which was robust and efficient even when differential evolution algorithm returned a solution far from the optimum. With the result as initial condition, we applied sequential least squares programming ([Kraft, 1988](#)), which

converged quickly to a neighbourhood of the respective likelihood maximum. Finally, we refined the result with a trust-region Newton-Raphson method (Nocedal & Wright, 2006), which is particularly efficient in the neighbourhood of the maximum. Only when we optimized the model for the day suitability, we skipped the L-BFGS-G and the sequential least squares programming step, because the model had a simple likelihood function and only few parameters, which made it easy to fit the model. For all applied algorithms, we used the implementations from the scientific computing library Scipy (Jones *et al.*, 2001).

Whenever needed, we determined derivatives of the log-likelihood functions via automatic differentiation. To that end, we used the python package “autograd”. However, some special functions in the log-likelihood function of the submodel for the choice parameters (see Appendix S3.3) were not included in the automatic differentiation package. Hence, we approximated derivatives numerically, using the package “numdifftools”.

To avoid numerical issues arising when optimizers step outside of the domain of the likelihood function, we mapped parameters to the domain as follows: when a parameter x was constrained to be positive, it was expressed as

$$x = \begin{cases} \exp \tilde{x} & \text{if } \tilde{x} < 0 \\ \tilde{x} + 1 & \text{else,} \end{cases} \quad (\text{S37})$$

and if it was constrained to the interval $[0, 1]$, it was expressed as

$$x = \frac{1}{\pi} \arctan \tilde{x} + \frac{1}{2}. \quad (\text{S38})$$

Then, the transformed unconstrained parameter \tilde{x} was optimized, respectively.

Most parameters we considered had a “natural” domain. For example, all parameters representing probabilities are constrained to the interval $[0, 1]$. However, the domain of the parameters of the gravity model used to estimate the angler activeness and the destination choice probabilities may be less clear. We constrained the “factor” parameters β_k (see equations (9) and (10) in the main text) to positive values to avoid the possibility to obtain negative trip rates. The “exponent” parameters γ_k were constrained to positive values if and only if the respective covariate included zeros or very small values. This was the case for all covariates referring to the subbasins.

S4.2 AIC optimization

Our gravity model for the angler activeness and the destination choice probabilities can involve a large number of parameters. Considering all possible combinations of parameters to select the model with the minimal AIC would not be feasible. However, the search can be sped with a branch and bound type search, which we describe below.

For a set \mathcal{P} of parameters let $\ell_{\mathcal{P}}^*$ be the maximal log-likelihood that can be achieved if these parameters are included in the model and $\text{AIC}_{\mathcal{P}}$ the corresponding AIC value. Suppose we have already determined the AIC value of some models, where AIC^* is the lowest AIC value we have achieved so far. Since we are considering nested models, exclusion of a parameter can never increase the likelihood. Hence, for any subset $\mathcal{P}' \subset \mathcal{P}$ it is $\ell_{\mathcal{P}'}^* \leq \ell_{\mathcal{P}}^*$. By definition of the AIC, it is

$$\text{AIC}_{\mathcal{P}} = 2(|\mathcal{P}| - \ell_{\mathcal{P}}^*), \quad (\text{S39})$$

where $|\mathcal{P}|$ denotes the number of elements in the set \mathcal{P} .

Let \mathfrak{P} be the set of all parameter sets that we have considered so far. Suppose $\mathcal{P}' \notin \mathfrak{P}$ is a parameter set that leads to a better AIC value than the currently best one: $\text{AIC}_{\mathcal{P}'} < \text{AIC}^*$. For any $\mathcal{P} \in \mathfrak{P}$ with $\mathcal{P}' \subset \mathcal{P}$ it holds then

$$\text{AIC}^* > 2(|\mathcal{P}'| - \ell_{\mathcal{P}'}^*) \geq 2(|\mathcal{P}'| - \ell_{\mathcal{P}}^*). \quad (\text{S40})$$

Thus,

$$|\mathcal{P}'| < \max_{\mathcal{P} \in \mathfrak{P}: \mathcal{P}' \subset \mathcal{P}} \ell_{\mathcal{P}}^* + \frac{1}{2} \text{AIC}^*, \quad (\text{S41})$$

and we can ignore all parameter combinations that do not satisfy this condition.

To minimize the AIC value, we start with the full model (including all possible parameters). Then, we consider all models for which one parameter is left out, then all models for which two parameters are left out and so on. In doing so, we skip all models that do not satisfy condition (S41) with the best currently found AIC value. We terminate the search when no admissible parameter set is left.

In the worst case, the search may include an extremely large number of models that cannot be considered in reasonable time. In practice, however, a certain set of parameters improves the model fit by a lot, so that only combinations in which the remaining parameters are left out need to be considered. Hence, a complete search is often possible in practice.

Since it would require an exponential number of computation steps to explicitly check for each possible

parameter combination whether condition (S41) is satisfied, this is not a viable option in practice. Instead, we store all already considered parameter sets in a trie data structure (Aoe, 1989), which enables us to efficiently generate only those parameter combinations that satisfy condition (S41). That way, a complete search remains feasible even if the a large number of parameters are considered.

S5 Computing the expected mean yearly fishing days per angler

Below, we show how the mean expected number of days that anglers in Alberta go fishing can be computed based on our model. Consider an angler from locality i . The number of their trips on a given day t is negative binomially distributed with mean $\mu_i\tau_t$ and dispersion parameter τ_t/α . Hence, the probability that they made at least one trip on day t is

$$\begin{aligned} \mathbb{P}(\text{\#trips on day } t \geq 1) &= 1 - \mathbb{P}(\text{\#trips on day } t = 0) \\ &= 1 - \left(\frac{1}{1 + \alpha\mu_i} \right)^{\frac{\tau_t}{\alpha}}. \end{aligned} \tag{S42}$$

Let \mathcal{T} be the set of days in the year of interest. Then the expected mean number of yearly fishing days is given by

$$\frac{\sum_i \sum_{t \in \mathcal{T}} n_i \left(1 - \left(\frac{1}{1 + \alpha\mu_i} \right)^{\frac{\tau_t}{\alpha}} \right)}{\sum_i n_i}. \tag{S43}$$

S6 The effect of an overestimated dispersion parameter on model estimates

In this appendix, we show how overestimating the dispersion parameter affects the estimated mean traffic counts. The dispersion parameter may be overestimated if no data replicates are available to fit the model (e.g. from a longitudinal study) and errors due to a misspecified model are mistakenly attributed to stochasticity. Piegorsch (1990) noted that the log-likelihood function for n independent samples y_i from a negative binomial distribution with dispersion parameter α and mean μ can be written as

$$\ell(\alpha, \mu) = \frac{1}{n} \sum_{i=1}^n \left(\sum_{\nu=0}^{y_i-1} \ln(1 + \alpha\mu) + y_i \ln \mu - (y_i + \alpha^{-1}) \ln(1 + \alpha\mu) \right), \tag{S44}$$

with partial derivative

$$\begin{aligned}\frac{\partial}{\partial \mu} \ell(\alpha, \mu) &= \frac{1}{n} \sum_{i=1}^n \left(\frac{y_i}{\mu} - \frac{1 + \alpha y_i}{1 + \alpha \mu} \right) \\ &= \frac{1}{n} \sum_{i=1}^n \frac{y_i - \mu}{\mu(1 + \alpha \mu)}.\end{aligned}\tag{S45}$$

Suppose that each observation y_i has been drawn from a distribution with different mean μ_i , which is computed based on a covariate vector c_i according to a model with parameter vector θ :

$$\mu_i = f(\theta; c_i).\tag{S46}$$

When the likelihood is maximized with respect to θ , the partial derivatives with respect to the components θ_j must be 0:

$$\begin{aligned}0 &= \frac{\partial}{\partial \theta_j} \ell(\alpha, \mu_1, \dots, \mu_n) \\ &= \sum_{i=1}^n \frac{\partial \mu_i}{\partial \theta_j} \frac{\partial \ell}{\partial \mu_i} \\ &= \frac{1}{n} \sum_{i=1}^n \frac{\partial \mu_i}{\partial \theta_j} \frac{y_i - \mu_i}{\mu_i(1 + \alpha \mu_i)}.\end{aligned}\tag{S47}$$

Clearly, if the model fits the data perfectly, then

$$\mu_i = y_i\tag{S48}$$

solves (S47) regardless of the value of α . However, if the model is slightly misspecified or (S48) cannot be achieved due to the stochastic nature of the observations y_i , the dispersion parameter has an effect on the estimates of the mean values μ_i . With small overdispersion, $\alpha \rightarrow 0$, equation (S47) becomes approximately

$$0 = \sum_{i=1}^n \frac{\partial \mu_i}{\partial \theta_j} \frac{y_i - \mu_i}{\mu_i},\tag{S49}$$

whereas we obtain with large overdispersion, $\alpha \rightarrow \infty$,

$$0 = \sum_{i=1}^n \frac{\partial \mu_i}{\partial \theta_j} \frac{y_i - \mu_i}{\mu_i^2}.\tag{S50}$$

That is, when fitting the model, values with small predicted mean are weighed higher if the overdispersion

is large. Consequently, if the dispersion parameter α is overestimated, estimates from the fitted model will match small values more accurately than large values. When estimating traffic flows, this is of two-fold concern: (1) Often, large traffic flows are of higher interest than small ones. Hence, it is of disadvantage when the model fits traffic flows with small mean better than traffic flows with high mean. (2) Since trips are rare events for weak traffic flows, the corresponding trip counts are subject to significant error. Unless a very large dataset is available, putting a disproportionate weight on these highly stochastic observations may lead to overfitting.

References

- Aoe, J.I. (1989) An efficient digital search algorithm by using a double-array structure. *IEEE Transactions on Software Engineering*, **15**, 1066–1077. doi: 10.1109/32.31365.
- Byrd, R.H., Lu, P., Nocedal, J. & Zhu, C. (1995) A limited memory algorithm for bound constrained optimization. *SIAM Journal on Scientific Computing*, **16**, 1190–1208. doi: 10.1137/0916069.
- Jones, E., Oliphant, T. & Peterson, P. (2001) SciPy: open source scientific tools for Python. Retrieved from <https://scipy.org/>.
- Kraft, D. (1988) A software package for sequential quadratic programming. Technical Report DFVLR-FB 88-28, DLR German Aerospace Center – Institute for Flight Mechanics, Köln, Germany.
- Nocedal, J. & Wright, S.J. (2006) Trust-region methods. *Numerical Optimization*, pp. 66–100. Springer New York, 2nd edition.
- Piegorsch, W.W. (1990) Maximum likelihood estimation for the negative binomial dispersion parameter. *Biometrics*, **46**, 863. doi: 10.2307/2532104.
- Storn, R. & Price, K. (1997) Differential evolution – a simple and efficient heuristic for global optimization over continuous spaces. *Journal of global optimization*, **11**, 341–359. doi: 10.1023/A:1008202821328.
- Villa, E.R. & Escobar, L.A. (2006) Using moment generating functions to derive mixture distributions. *The American Statistician*, **60**, 75–80. doi: 10.1198/000313006X90819.